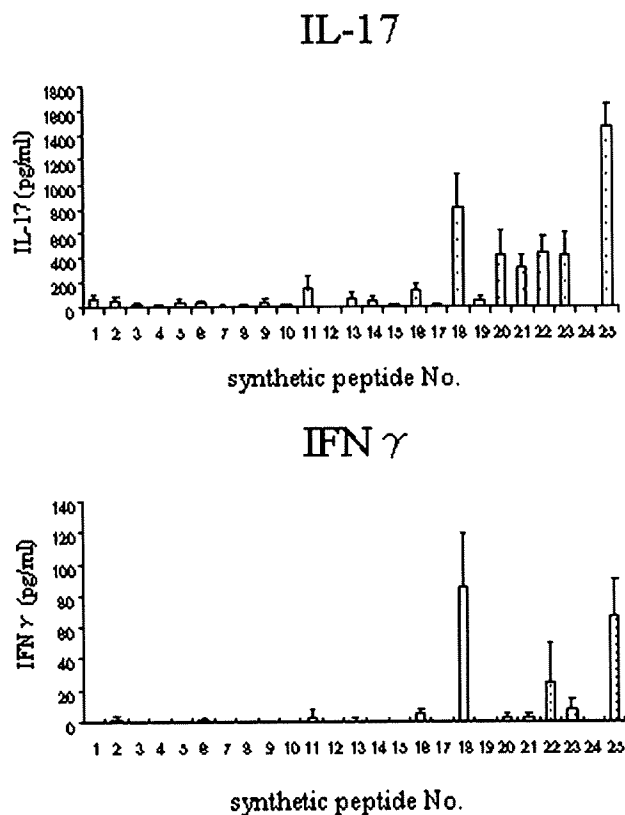


Figure 1



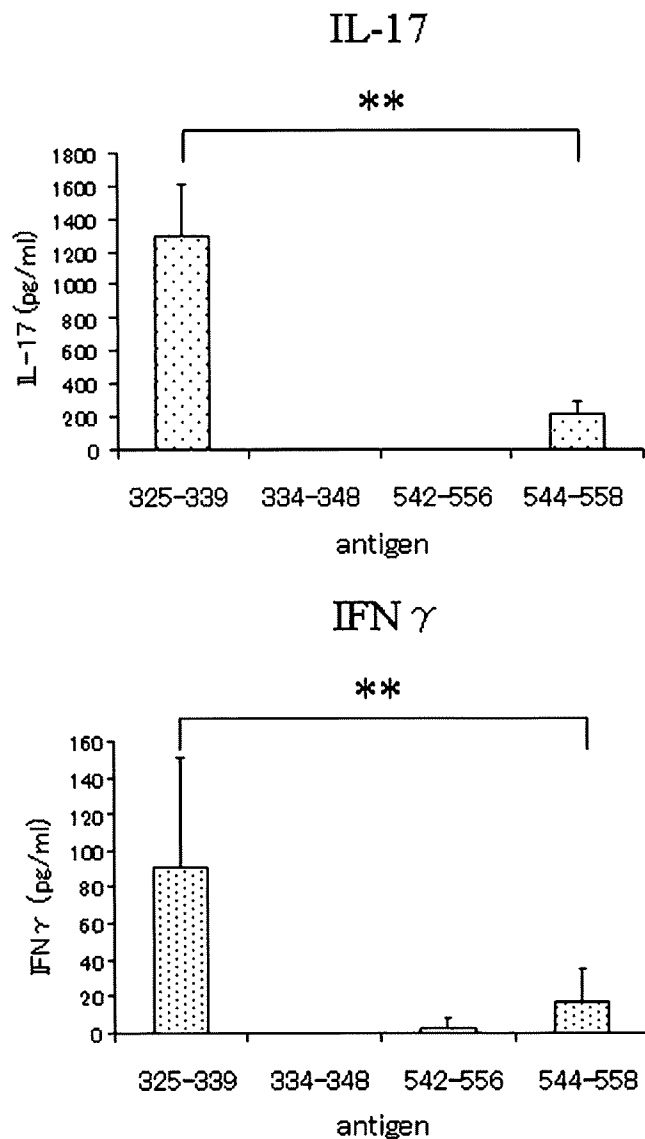
Synthetic peptides number 18 and 25 produced marked simulation of glucose-6-phosphate isomerase (GPI) primed CD4⁺ T cells. Mice were sacrificed on day 7 after immunisation. CD4⁺ T cells were purified from spleen cells of GPI-immunised DBA/1 mice. GPI-primed CD4⁺ T cells and antigen presenting cells (APCs) were co-cultured with 10 μ M of synthetic peptide for 24 hours. The supernatants were assayed for interferon (IFN) γ and interleukin (IL) 17 by ELISA. Data are averages \pm standard deviation of three culture wells. Representative data of three independent experiments.

cross-reactivity with mouse GPI might be the pathogenesis of peptide-induced arthritis.

Immunisation of human GPI₃₂₅₋₃₃₉ leads B cells to produce anti-mouse GPI antibodies

To explore the importance of autoantibodies, we measured anti-human GPI antibodies and anti-mouse GPI antibodies in mice immunised with hGPI₃₂₅₋₃₃₉, hGPI₅₄₄₋₅₅₈ and hGPI₃₂₅₋₃₃₉ plus hGPI₅₄₄₋₅₅₈ by ELISA. Mice immunised with rhGPI and the two peptides (hGPI₃₂₅₋₃₃₉ plus hGPI₅₄₄₋₅₅₈) produced high titres of anti-human GPI antibodies and anti-mouse GPI antibodies, and mice immunised with hGPI₃₂₅₋₃₃₉ and hGPI₅₄₄₋₅₅₈ hardly produced any anti-human GPI antibodies. However, mice immunised with hGPI₃₂₅₋₃₃₉ produced significantly higher titres of anti-mouse GPI antibodies than mice immunised with hGPI₅₄₄₋₅₅₈ (Figure 6a). It is noteworthy that immunisation with the two peptides (hGPI₃₂₅₋₃₃₉ plus hGPI₅₄₄₋₅₅₈) induced significantly higher titres of anti-mouse

Figure 2



GPI₃₂₅₋₃₃₉ is a major epitope. Mice were sacrificed on day 7 after immunisation. CD4⁺ T cells were purified from splenocytes of glucose-6-phosphate isomerase (GPI) immunised DBA/1 mice. GPI-primed CD4⁺ T cells and antigen presenting cells (APCs) were co-cultured with 10 μ M of synthetic peptide hGPI₃₂₅₋₃₃₉, hGPI₃₃₄₋₃₄₈, hGPI₅₄₂₋₅₅₆ or hGPI₅₄₄₋₅₅₈ for 24 hours. The purity of each peptide was 90%. The supernatants were assayed for interferon (IFN) γ and interleukin (IL) 17 by ELISA. Data are averages \pm standard deviation of five culture-wells. **p < 0.01 (Mann-Whitney's U test). Representative data of three independent experiments.

GPI antibodies than that with hGPI₃₂₅₋₃₃₉ alone, whereas the severity and incidence of arthritis in mice immunised with two peptides (hGPI₃₂₅₋₃₃₉ plus hGPI₅₄₄₋₅₅₈) were comparable with those in mice immunised with hGPI₃₂₅₋₃₃₉ alone (Figures 3a and 6a).

Table 4**Re-synthesised peptides used for determining a major epitope**

Peptide number	Peptide	Synthetic peptide sequence
18	327-346	H-Y <u>I</u> N <u>C</u> F <u>G</u> C <u>E</u> T <u>H</u> A <u>M</u> L <u>P</u> <u>Y</u> D <u>Q</u> <u>Y</u> L <u>H</u> -OH
	325-339	H-I <u>W</u> <u>Y</u> <u>I</u> <u>N</u> <u>C</u> <u>F</u> <u>G</u> <u>C</u> <u>E</u> <u>T</u> <u>H</u> A <u>M</u> L-OH
	334-348	H-E <u>T</u> <u>H</u> A <u>M</u> L <u>P</u> <u>Y</u> D <u>Q</u> <u>Y</u> L <u>H</u> R <u>F</u> -OH
25	539-558	H-D <u>A</u> S <u>T</u> <u>N</u> <u>G</u> L <u>I</u> <u>N</u> <u>F</u> <u>I</u> <u>K</u> <u>Q</u> <u>Q</u> R <u>E</u> A <u>R</u> <u>V</u> <u>Q</u> -OH
	542-556	H-T <u>N</u> <u>G</u> L <u>I</u> <u>N</u> <u>F</u> <u>I</u> <u>K</u> <u>Q</u> <u>Q</u> R <u>E</u> A <u>R</u> -OH
	544-558	H-G <u>L</u> <u>I</u> <u>N</u> <u>F</u> <u>I</u> <u>K</u> <u>Q</u> <u>Q</u> R <u>E</u> A <u>R</u> <u>V</u> <u>Q</u> -OH

The 15-mer peptides were synthesised with 90% purity, containing each core sequence of number 18 peptide (GPI₃₂₇₋₃₄₆) and number 25 peptide (GPI₅₃₉₋₅₅₈). Amino acid residues constituting the core sequence and those thought to bind the anchors of I-A^g are underlined and shown in bold letters, respectively.

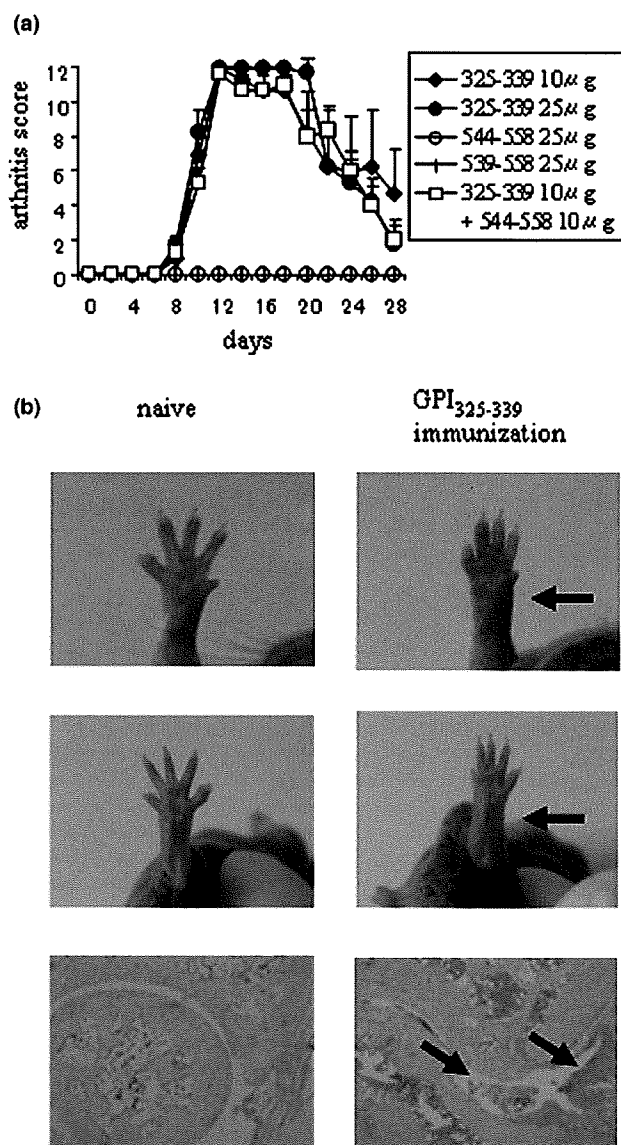
We further investigated the difference of the correlation between anti-mouse GPI antibodies and arthritis score among immunisation patterns. Each of the three different immunisation patterns (rhGPI, hGPI₃₂₅₋₃₃₉ and hGPI₃₂₅₋₃₃₉ plus hGPI₅₄₄₋₅₅₈) showed no positive correlation between anti-mouse GPI antibodies and arthritis score (Table 5).

Next, we investigated the existence of IgG on the cartilage surface by immunohistology, because GPI were proved to deposit on the cartilage surface of normal naïve mice [23]. The cryostat sections of ankle joints from naïve mice and mice immunised with hGPI₅₄₄₋₅₅₈ did not show IgG deposit on the cartilage surface. However, those from mice immunised with rhGPI and hGPI₃₂₅₋₃₃₉ showed IgG deposits (Figure 6b). These data indicate that anti-mouse GPI antibodies may play a role in the development of peptide-induced arthritis.

Discussion

GPI, a ubiquitous glycolytic enzyme, is a new autoantigen candidate in autoimmune arthritis [5,6]. GPI-induced arthritis is induced by immunisation of genetically unaltered DBA/1 mice with rhGPI [1]. We report here the therapeutic efficacies of mAb to tumour necrosis factor- α and IL-6 and CTLA-4 Ig in this model [3]. Moreover, CD4⁺ T cells, especially Th17 cells, seem to be more important than B cells, because administration of anti-CD4 mAb or anti-IL-17 mAb markedly ameliorate the progress of arthritis independent of anti-GPI antibodies titres [1,2]. Therefore, exploring the epitope of CD4⁺ T cells and its arthritogenic effect is important for understanding the pathological mechanisms.

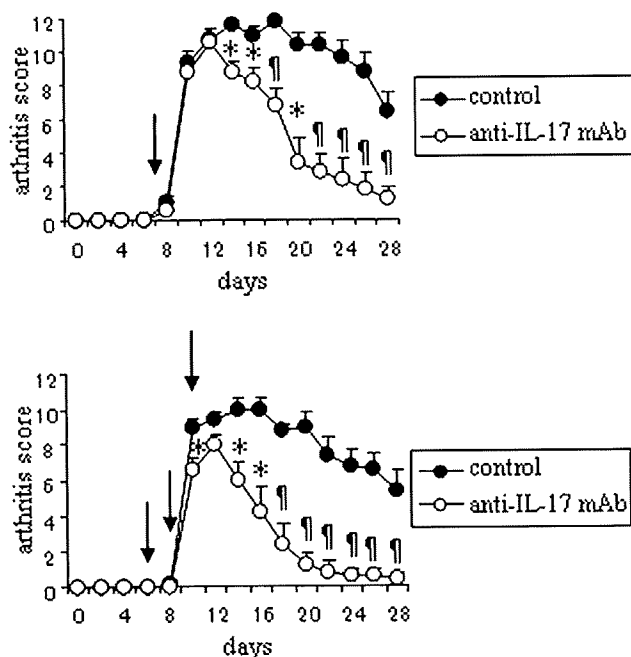
In this study, we investigated the binding motif of I-A^g from T cell epitopes considered to bind to I-A^g, synthesised peptides of epitope candidates and identified hGPI₃₂₅₋₃₃₉ as a major epitope. Interestingly, the MHC binding residues of hGPI₃₂₅₋₃₃₉(IWYINCFGCETHAML) at P1, P4 and P7 were the same as those for bovine CII₂₅₆₋₂₇₀ (GEP-

Figure 3

Immunisation with hGPI₃₂₅₋₃₃₉ induces severe polyarthritis. DBA/1 mice were immunised with 25 μg of hGPI₃₂₅₋₃₃₉, hGPI₅₃₉₋₅₅₈ or hGPI₅₄₄₋₅₅₈, or 10 μg each of hGPI₃₂₅₋₃₃₉ plus hGPI₅₄₄₋₅₅₈, and 200 ng of pertussis toxin was injected intraperitoneally on days 0 and 2 after immunisation. (a) The mean arthritis score (\pm standard error of the mean (SEM)) of five mice in one representative experiment of two independent experiments. (b) Severe swelling of the wrist (upper panels) and ankle joints (middle panels) in mice immunised with 25 μg of hGPI₃₂₅₋₃₃₉ compared with naïve mice (arrowheads). Histological analysis of haematoxylin & eosin-stained sections of ankle joints taken from naïve mice and mice on day 14 after hGPI₃₂₅₋₃₃₉ immunization (lower panels) showed severe synovitis with massive infiltration of cells and hyperplasia of synovial tissue (arrowheads).

induced arthritis [4]. These findings indicate that the binding motif (P1 I, P4 F, P7 E) might have high binding affinity with I-A^g, and the peptides with this motif-MHC complexes might be effectively recognised by TCRs and could be arthritogenic in some condition. Although immunisation with a fragment of

Figure 4



Anti-IL-17 monoclonal antibody (mAb) suppresses the development of arthritis. DBA/1 mice were immunised with 25 μ g of hGPI₃₂₅₋₃₃₉, and 200 ng of pertussis toxin was injected intraperitoneally on days 0 and 2 after immunisation. 100 μ g of anti-IL-17 mAb or isotype control (control) was administered intraperitoneally on day 7 (upper panel) or day 6, 8, and 10 (lower panel) after immunisation (arrow). Mean arthritis score (\pm standard error of the mean (SEM)) of five mice per group. Representative data of two independent experiments. * $p < 0.05$, † $p < 0.01$ (Mann-Whitney's U test).

cyanogen bromide of bovine CII, CB11 (CII₁₂₄₋₄₀₂), which contains the dominant epitope, can induce arthritis, the severity and incidence are much lower than arthritis induced by bovine CII protein [4]. Other fragments (CB8, CB9, CB10 and CB12) do not induce arthritis, as is explained by the production of anti-bovine CII antibodies. Immunisation with CB11 fragment produces five times more antibodies to bovine CII than any other fragment [4]. The observation that administration of anti-CD4 mAb after the onset of arthritis did not ameliorate the arthritis [24,25] and a combination of mAb to CII can passively transfer arthritis to naïve mice [26] also emphasises the importance of autoantibodies to the induction of collagen-induced arthritis.

Our study demonstrated that immunisation with hGPI₃₂₅₋₃₃₉ induced antigen-specific Th17 cells, which can cross-react with mGPI₃₂₅₋₃₃₉ and lead B cells to produce anti-mouse GPI antibodies. However, immunisation with hGPI₅₄₄₋₅₅₈ could not even induce hGPI₅₄₄₋₅₅₈-specific Th17 cells. The difference of ability of Th17 induction between two peptides may come from MHC-binding affinity and TCR-binding affinity. A peptide that is likely to bind to MHC class II with high affinity and interacts strongly with the T cell receptor tends to stimulate Th1-

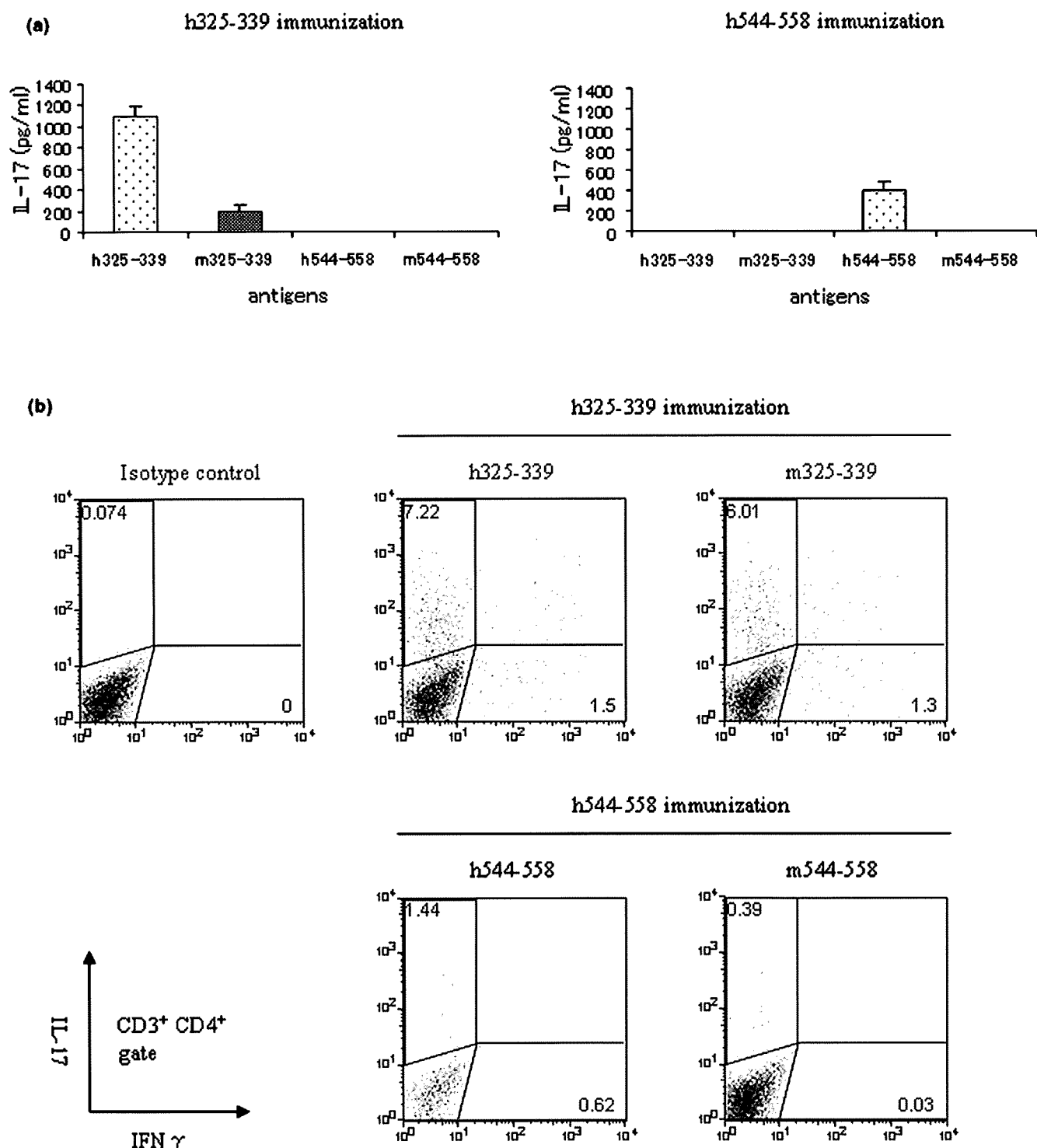
cell response, whereas a peptide with low binding affinity to MHC class II and T cell receptor tends to elicit Th2-cell response [27,28]. Although the relationship between Th17 differentiation and the strength of TCR signalling and MHC-binding affinity has not been clarified, it is possible that the difference in amino acid sequences between hGPI₃₂₅₋₃₃₉ and hGPI₅₄₄₋₅₅₈ might affect the I-A_g binding affinity and the TCR signalling, and consequently lead to the difference in extent of antigen-specific Th17 cells. In this study, we did not detect any IL-4 production, which is an adjuvant effect of *Mycobacterium tuberculosis* and pertussis toxin.

In K/BxN mice expressing I-A_g⁷ as MHC class II molecules, mGPI₂₈₂₋₂₉₄-specific CD4⁺ T cells lead B cells to produce anti-mouse GPI antibodies [16]. The anti-mouse GPI antibodies from K/BxN mice have such high affinity that IgG transfer of K/BxN mice can provoke arthritis in normal mice [6]. In comparison, the anti-mouse GPI antibodies from GPI-induced arthritis alone are not sufficient for the development of arthritis because IgG transfer from mice immunised with rhGPI can not provoke arthritis. However, IgG signalling through Fc γ R seems necessary for the induction of GPI-induced arthritis because Fc γ R-deficient mice are resistant to arthritis [1]. Moreover, the data that transfer of rhGPI-primed or hGPI₃₂₅₋₃₃₉-primed Th17 cells to naïve DBA/1 mice can not induce arthritis emphasises the necessity of anti-mouse GPI antibodies (unpublished observation). Considering the data that there are no positive correlation between anti-mouse GPI antibodies and arthritis score [[29] and unpublished observation], and arthritis-resistant mice like C57BL/6 produce as high titres of anti-mouse GPI antibodies as DBA/1 when immunised with rhGPI (1 and unpublished observation), anti-mouse GPI antibodies may play a subordinate role in the development of GPI-induced arthritis and peptide-induced arthritis in DBA/1 mice.

In the process of epitope screening, the response to hGPI₅₃₉₋₅₅₈ peptide was comparable with that to hGPI₃₂₇₋₃₄₆ peptide; however, the response to hGPI₅₄₂₋₅₅₆ and hGPI₅₄₄₋₅₅₈, which were synthesised with 90% purity, was lower than that to hGPI₅₃₉₋₅₅₈ peptide. Furthermore, the response to hGPI₅₃₉₋₅₅₈, which was re-synthesised with 90% purity, was much lower than to hGPI₃₂₅₋₃₃₉ or to hGPI₅₃₉₋₅₅₈ peptide for screening (data not shown). These results could be explained by differences in the purity of the synthetic peptides. The synthetic peptides used for screening (peptides numbers 1 to 25, Table 2) were unpurified, and the purity of each peptide would have been quite different, although the exact purity was unchecked by the product maker. Therefore, it is possible that the purity of number 25 peptide might have been much higher than that of number 18 peptide, or alternatively, number 25 peptide may have contained other peptides through peptide synthesis.

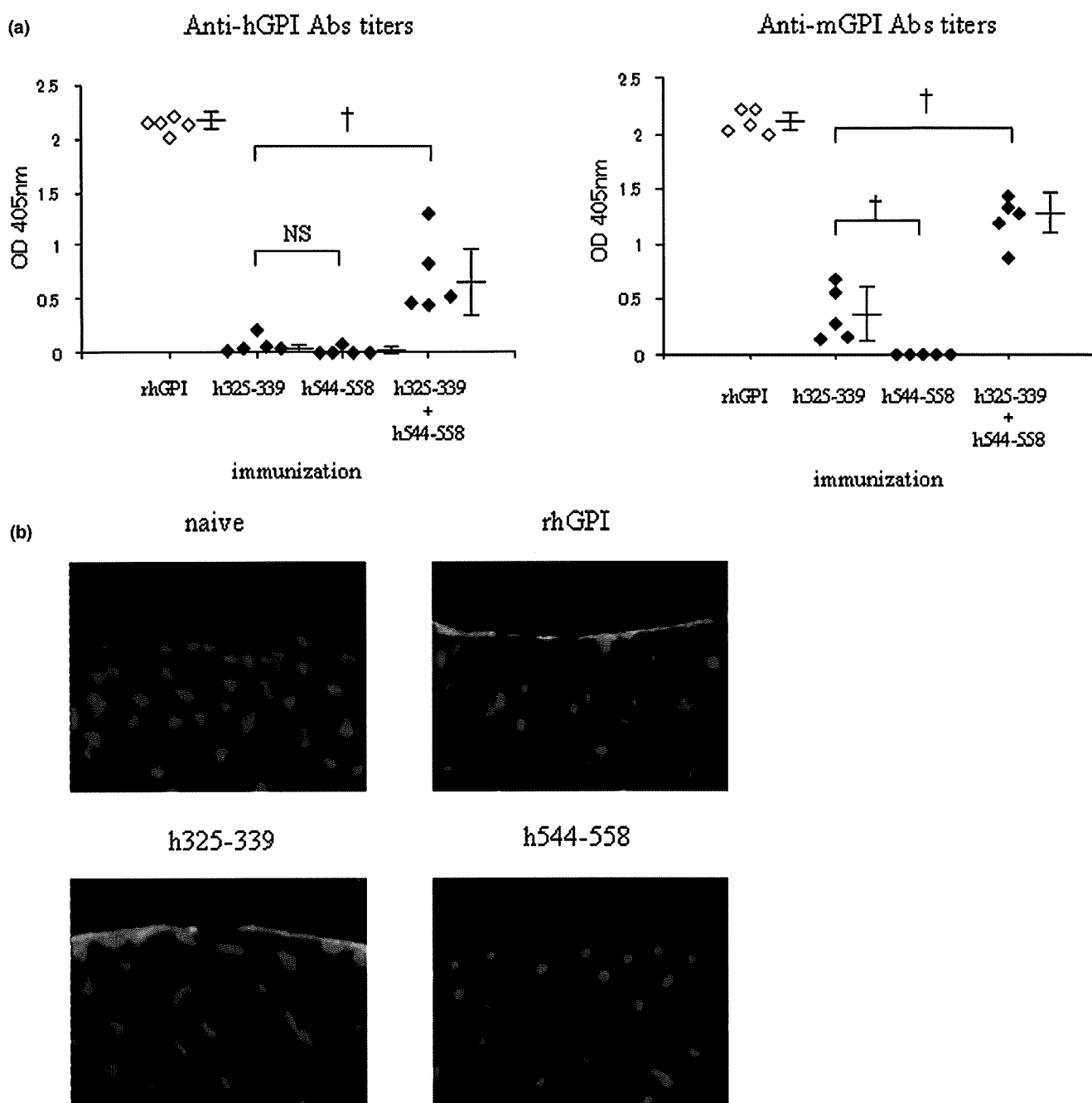
From a probability point of view, it is possible that other epitopes exist in some regions of human GPI-amino acid

Figure 5



Cross-reactivity with peptides derived from mouse glucose-6-phosphate isomerase (GPI). (a) Draining lymph node (DLN) cells taken from hGPI₃₂₅₋₃₃₉-immunised mice on day 5 were cultured with 10 μ M of hGPI₃₂₅₋₃₃₉, mGPI₃₂₅₋₃₃₉, hGPI₅₄₄₋₅₅₈ or mGPI₅₄₄₋₅₅₈ for 24 hours. The supernatants were assayed for interleukin (IL) 17 by ELISA. Data are averages \pm standard deviation of three culture-wells. Representative data of three independent experiments. (b) DLN cells taken from hGPI₃₂₅₋₃₃₉⁻ or hGPI₅₄₄₋₅₅₈⁻ immunised mice on day 5 were cultured with 10 μ M of hGPI₃₂₅₋₃₃₉ and mGPI₃₂₅₋₃₃₉ or hGPI₅₄₄₋₅₅₈ and mGPI₅₄₄₋₅₅₈, respectively. GoldiStop was added at the last four hours of each culture. Flow cytometry for IL-17 and interferon (IFN) γ was gated in CD3⁺, CD4^{high} cells. Representative flow cytometry data of three independent experiments with two mice per experiment.

Figure 6



Titres of anti-mouse glucose-6-phosphate isomerase (GPI) antibodies were elevated in mice with arthritis. (a) Sera were taken on day 14 from mice immunised with recombinant human (rh) GPI, hGPI₃₂₅₋₃₃₉, hGPI₅₄₄₋₅₅₈ or hGPI₃₂₅₋₃₃₉ plus hGPI₅₄₄₋₅₅₈, and the titres of anti-human GPI antibodies and anti-mouse GPI antibodies were analysed by ELISA. Each symbol represents a single mouse. Data are mean optimal density \pm standard deviation. $\dagger p < 0.01$ (Mann-Whitney's U test). Representative data of two independent experiments. (b) Ankle joints were taken on day 14 from mice immunised with rhGPI, hGPI₃₂₅₋₃₃₉ or hGPI₅₄₄₋₅₅₈. Cryostat sections of ankle joints were stained with anti-mouse IgG (red), and nuclei were counterstained with 4',6-diamidino-2-phenylindole dilactate (blue). Representative data of three independent experiments.

sequence from which we did not synthesise the peptides, because I-A^g may have another binding motif and our synthesised peptides covered only the 399/558 (71.5%) amino acid residues of human GPI protein, not the whole length. However, two experimental pieces of data support that hGPI₃₂₅₋₃₃₉

may be the dominant epitope. One is that immunisation with hGPI₃₂₅₋₃₃₉ provoked arthritis similar to that induced by rhGPI protein. The other is that intraperitoneal injection of hGPI₃₂₅₋₃₃₉ after the onset of arthritis significantly ameliorated the progress of arthritis (data not shown). Because systemic

Table 5**Correlation between anti-mouse glucose-6-phosphate isomerase (GPI) antibodies titres and arthritis score**

Immunisation	Rho value	P value
rhGPI	-0.825	0.0989
h325-339	-0.525	0.2937
h325-339 plus h544-558	0.500	0.3173

Sera were taken on day 14 from mice immunised with recombinant human (rh) GPI, hGPI₃₂₅₋₃₃₉ or hGPI₃₂₅₋₃₃₉ plus hGPI₅₄₄₋₅₅₈. The correlation between the titres of anti-GPI antibodies and arthritis score on day 14 were statistically analysed with the Spearman's rank correlation coefficient. In the case of five samples, Rho values above 0.900 indicate significant positive correlation between anti-mouse GPI antibody titres and arthritis score, whereas Rho values below -0.900 indicate significant negative correlation ($p < 0.05$). Five mice per group. Representative data of two independent experiments.

administration of a dominant epitope leads to anergy of pathogenic T cells or results in activation-induced cell death [30,31], this inhibitory effect of hGPI₃₂₅₋₃₃₉ on GPI-induced arthritis supports the notion that hGPI₃₂₅₋₃₃₉ may be the dominant epitope.

Cross-reactivity is considered the one of mechanisms of autoimmune diseases. We previously identified patients with RA who have GPI-reactive CD4⁺ T cells and found that some of them express human leucocyte antigen-DR4 as MHC class II [32]. Because the I-A^g binding motif resembles DR4 [9], further studies are needed to define epitopes of CD4⁺ T cells in such patients and search proteins that have homology to the epitopes.

Conclusions

This study is the first report of experimental arthritis induced by immunisation with a single short peptide in genetically unaltered mice. The fact that an immunological reaction to a single short peptide of ubiquitously expressed protein causes polyarthritis provides new insight to the understanding of autoimmune arthritis.

Competing interests

The authors declare that they have no competing interests.

Authors' contributions

KI wrote the manuscript and conceived of the study. YT and AI assisted experiments and statistical analysis. IM and TS participated in its full design and coordination, and DG, SI and AK participated in discussions.

Acknowledgements

This work was supported in part by a grant from The Japanese Ministry of Science and Culture (IM, TS).

References

- Schubert D, Maier B, Morawietz L, Krenn V, Kamradt T: Immunization with glucose-6-phosphate isomerase induces T cell-dependent peripheral polyarthritis in generally unaltered mice. *J Immunol* 2004, **172**:4503-4509.
- Iwanami K, Matsumoto I, Tanaka-Watanabe Y, Mihira M, Ohsugi Y, Mamura M, Goto D, Ito S, Tsutsumi A, Kishimoto T, Sumida T: Crucial role of IL-6/IL-17 axis in the induction of arthritis by glucose-6-phosphate isomerase. *Arthritis Rheum* 2008, **58**:754-763.
- Matsumoto I, Zhang H, Yasukochi T, Iwanami K, Tanaka Y, Inoue A, Goto D, Ito S, Tsutsumi A, Sumida T: Therapeutic effects of antibodies to tumor necrosis factor- α , interleukin-6 and cytotoxic T-lymphocyte antigen 4 immunoglobulin in mice with glucose-6-phosphate isomerase induced arthritis. *Arthritis Res Ther* 2008, **10**:R66.
- Brand DD, Myers LK, Terato K, Whittington KB, Stuart JM, Kang AH, Rosloniec EF: Characterization of the T cell determinants in the induction of autoimmune arthritis by bovine α 1(II)-CB11 in H-2^a mice. *J Immunol* 1994, **152**:3088-3097.
- Matsumoto I, Lee DM, Goldbach-Mansky R, Sumida T, Hitchon CA, Schur PH, Anderson RJ, Coblyn JS, Weinblatt ME, Brenner M, Duclos B, Pasquali JL, El-Gabalawy H, Mathis D, Benoist C: Low prevalence of antibodies to glucose-6-phosphate isomerase in patients with rheumatoid arthritis and a spectrum of other chronic autoimmune disorders. *Arthritis Rheum* 2003, **48**:944-954.
- Matsumoto I, Staub A, Benoist C, Mathis D: Arthritis provoked by linked T and B recognition of a glycolytic enzyme. *Science* 1999, **286**:1732-1735.
- MHCPred (<http://www.jenner.ac.uk/MHCPred/>)
- Kawamoto T: Use of a new adhesive film for the preparation of multi-purpose fresh-frozen sections from hard tissues, whole-animals, insects and plants. *Arch Histol Cytol* 2003, **66**:123-143.
- Bayrak S, Holmdahl R, Travers P, Lauster R, Hesse M, Dölling R, Mitchison NA: T cell response of I-A^g mice to self type II collagen: meshing of the binding motif of the I-A^g molecule with repetitive sequences results in autoreactivity to multiple epitopes. *Int Immunol* 1997, **9**:1687-1699.
- Chen JS, Lorenz RG, Goldberg J, Allen PM: Identification and characterization of a T cell-inducing epitope of bovine ribonuclease that can be restricted by multiple class II molecules. *J Immunol* 1991, **147**:3672-3678.
- Fritz RB, Skeen MJ, Chou CH, Garcia M, Egorov IK: Major histocompatibility complex-linked control of the murine immune response to myelin basic protein. *J Immunol* 1985, **134**:2328-2332.
- Sakai K, Sinha AA, Mitchell DJ, Zamvil SS, Rothbard JB, McDevitt HO, Steinmann L: Involvement of distinct murine T-cell receptors in the autoimmune encephalitogenic response to nested epitopes of myelin basic protein. *Proc Natl Acad Sci USA* 1988, **85**:8608-8612.
- Myers LK, Cooper SW, Terato K, Seyer JM, Stuart JM, Kang AH: Identification and characterization of a tolerogenic T cell determinant within residues 181-209 of chick type II collagen. *Clin Immunol Immunopathol* 1995, **75**:33-38.
- Michaëlsson E, Andersson M, Engström A, Holmdahl R: Identification of an immunodominant type-II collagen peptide recognized by T cells in H-2^a mice: self tolerance at the level of determinant selection. *Eur J Immunol* 1992, **22**:1819-1825.
- Myers LK, Seyer JM, Stuart JM, Terato K, David CS, Kang AH: T cell epitopes of type II collagen that regulate murine collagen-induced arthritis. *J Immunol* 1993, **151**:500-505.
- Basu D, Horvarh S, Matsumoto I, Fremont DH, Allen PM: Molecular basis for recognition of an arthritic peptide and a foreign epitope on distinct MHC molecules by a single TCR. *J Immunol* 2000, **164**:5788-5796.
- Bettelli E, Carrier Y, Gao W, Korn T, Strom TB, Oukka M, Weiner HL, Kuchroo VK: Reciprocal development pathways for the generation of pathogenic effector T_H17 and regulatory T cells. *Nature* 2006, **441**:235-238.
- Mangan PR, Harrington LE, O'Quinn DB, Helms WS, Bullard DC, Elson CO, Hatton RD, Wahl SM, Schoeb TR, Weaver CT: Transforming growth factor-beta induces development of the T (H) 17 lineage. *Nature* 2006, **441**:231-234.
- He D, Wu L, Kim HK, Li H, Elmets CA, Xu H: CD8⁺ IL-17 producing T cells are important effector functions for the elicitation of contact hypersensitivities responses. *J Immunol* 2006, **177**:6852-6858.

20. Michel ML, Keller AC, Paget C, Fujio M, Trottein F, Savage PB, Wong CH, Schneider E, Dy M, Leite-de-Moraes MC: **Identification of an IL-17-producing NK1.1neg iNKT cell population involved in airway neutrophilia.** *J Exp Med* 2007, **204**:995-1001.
21. Yoshiga Y, Goto D, Segawa S, Ohnishi Y, Matsumoto I, Ito S, Tsutsumi A, Taniguchi M, Sumida T: **Invariant NKT cells produce IL-17 through IL-23-dependent and -independent pathways with potential modulation of Th17 response in collagen-induced arthritis.** *Int J Mol Med* 2008, **22**:369-374.
22. Lockhart E, Green AM, Flynn JL: **IL-17 production is dominated by gammadelta T cells rather than CD4 T cells during Mycobacterium tuberculosis infection.** *J Immunol* 2006, **177**:4662-4669.
23. Matsumoto I, Maccioni M, Lee DM, Maurice M, Simmons B, Brenner M, Mathis D, Benoist C: **How antibodies to a ubiquitous cytoplasmic enzyme may provoke joint-specific autoimmune disease.** *Nat Immunol* 2002, **3**:360-365.
24. Ranges GE, Sriram S, Cooper SM: **Prevention of type II collagen-induced arthritis by in vivo treatment with anti-L3T4.** *J Exp Med* 1985, **162**:1105-1110.
25. Williams RO, Whyte A: **Anti-CD4 monoclonal antibodies suppress murine collagen-induced arthritis only at the time of primary immunization.** *Cell Immunol* 1996, **170**:291-295.
26. Terato K, Harper DS, Griffiths MM, Hasty DL, Ye XJ, Cremer MA, Seyer JM: **Collagen-induced arthritis in mice: synergistic effect of E. coli lipopolysaccharide bypasses epitope specificity in the induction of arthritis with monoclonal antibodies to type II collagen.** *Autoimmunity* 1995, **22**:137-147.
27. Constant S, Pfeiffer C, Woodard A, Pasqualini T, Bottomly K: **Extent of T cell receptor ligation can determine the functional differentiation of naive CD4+ T cells.** *J Exp Med* 1995, **182**:1591-1596.
28. Leitenberg D, Boutin Y, Constant S, Bottomly K: **CD4 regulation of TCR signaling and T cell differentiation following stimulation with peptides of different affinities for the TCR.** *J Immunol* 1998, **161**:1194-1203.
29. Bockermann R, Schubert D, Kamradt T, Holmdahl R: **Induction of a B-cell-dependent chronic arthritis with glucose-6-phosphate isomerase.** *Arthritis Res Ther* 2005, **7**:R1316-R1324.
30. Critchfield JM, Racke MK, Zúñiga-Pflücker JC, Cannella B, Raine CS, Goverman J, Lenardo MJ: **T cell deletion in high antigen dose therapy of autoimmune encephalomyelitis.** *Science* 1994, **263**:1139-1143.
31. Gaur A, Wiers B, Liu A, Rothbard J, Fathman CG: **Amelioration of autoimmune encephalomyelitis by myelin basic protein synthetic peptide-induced anergy.** *Science* 1992, **258**:1491-1494.
32. Kori Y, Matsumoto I, Zhang H, Yasukochi T, Hayashi T, Iwanami K, Goto D, Ito S, Tsutsumi A, Sumida T: **Characterisation of Th1/Th2 type, glucose-6-phosphate isomerase reactive T cells in the generation of rheumatoid arthritis.** *Ann Rheum Dis* 2006, **65**:968-969.

Comprehensive Gene Expression Profiling of Peyer's Patch M Cells, Villous M-Like Cells, and Intestinal Epithelial Cells¹

Kazutaka Terahara,^{2*‡} Masato Yoshida,^{2*†} Osamu Igarashi,^{*‡} Tomonori Nochi,^{*‡} Gemilson Soares Pontes,^{*} Koji Hase,[§] Hiroshi Ohno,[§] Shiho Kurokawa,^{*} Mio Mejima,^{*} Naoko Takayama,^{*†} Yoshikazu Yuki,^{*‡} Anson W. Lowe,[¶] and Hiroshi Kiyono^{3*†‡}

Separate populations of M cells have been detected in the follicle-associated epithelium of Peyer's patches (PPs) and the villous epithelium of the small intestine, but the traits shared by or distinguishing the two populations have not been characterized. Our separate study has demonstrated that a potent mucosal modulator cholera toxin (CT) can induce lectin *Ulex europaeus* agglutinin-1 and our newly developed M cell-specific mAb NKM 16-2-4-positive M-like cells in the duodenal villous epithelium. In this study, we determined the gene expression of PP M cells, CT-induced villous M-like cells, and intestinal epithelial cells isolated by a novel approach using FACS. Additional mRNA and protein analyses confirmed the specific expression of glycoprotein 2 and myristoylated alanine-rich C kinase substrate (MARCKS)-like protein by PP M cells but not CT-induced villous M-like cells. Comprehensive gene profiling also suggested that CT-induced villous M-like cells share traits of both PP M cells and intestinal epithelial cells, a finding that is supported by their unique expression of specific chemokines. The genome-wide assessment of gene expression facilitates discovery of M cell-specific molecules and enhances the molecular understanding of M cell immunobiology. *The Journal of Immunology*, 2008, 180: 7840–7846.

As a unique epithelial cell type specializing in Ag sampling, microfold or membranous cells (M cells) are present in the follicle-associated epithelium (FAE)⁴ of both GALT and nasopharynx-associated lymphoid tissue, which act as a major inductive site for Ag-specific mucosal immune responses (1, 2). Recently, we also identified M cells in the small intestinal villous epithelium, at effector sites far from the FAE, suggesting that Ag sampling via villous M cells may be responsible for induction of systemic Ag-specific immune responses, such as IgG production via the oral route (3). Still missing, however, were a characterization of the shared and distinctive traits of Peyer's patches (PPs) and villous M cells and a better understanding of the immunological nature of each.

Recent comprehensive gene expression analyses using microdissected FAE or whole cells dissociated from the FAE identified genes specifically expressed by PP M cells (4–6). Similar data, however, have not been available for villous M cells, in part because sufficient numbers of M cells are difficult to isolate from the surrounding intestinal epithelial cells (IECs). In mice, lectin *Ulex europaeus* agglutinin-1 (UEA-1) possessing affinity for α (1, 2) fucose has been routinely used for the detection of such M cells (3, 7). UEA-1, however, does not alone suffice to identify M cells because it also reacts to goblet cells (3). Our laboratory has recently succeeded in distinguishing M cells from goblet cells by developing a mAb (NKM 16-2-4 mAb) that specifically reacts to murine PP and villous M cells but not goblet cells and IECs (8). Furthermore, our recent separate studies have demonstrated that oral administration of cholera toxin (CT) as mucosal adjuvant resulted in the induction of NKM 16-2-4 mAb⁺ and UEA-1⁺ M-like cells, which have pocket structure and Ag uptake ability, in the duodenal villous epithelium (Terahara et al., submitted for publication). These recent advances in our understanding of M cells allowed us to define gene expression profiles capable of distinguishing PP M cells, CT-induced villous M-like cells, and IECs.

*Division of Mucosal Immunology, Department of Microbiology and Immunology, The Institute of Medical Science and [†]Department of Medical Genome Science, Graduate School of Frontier Science, The University of Tokyo, Tokyo, [‡]Core Research for Evolutional Science and Technology, Japan Science and Technology Corporation, Saitama, and [§]Laboratory of Epithelial Immunobiology, Research Center for Allergy and Immunology, Institute of Physical and Chemical Research, Yokohama, Japan; and [¶]Department of Medicine, Stanford University, Stanford, CA 94305

Received for publication February 12, 2007. Accepted for publication April 3, 2008.

The costs of publication of this article were defrayed in part by the payment of page charges. This article must therefore be hereby marked *advertisement* in accordance with 18 U.S.C. Section 1734 solely to indicate this fact.

¹ This work was supported in part by grants from Core Research for Evolutional Science and Technology of the Japan Science and Technology Corporation, the Ministry of Education, Science, Sports, and Culture, and the Ministry of Health and Welfare in Japan.

² K.T. and M.Y. contributed equally to this work and share first authorship.

³ Address correspondence and reprint requests to Dr. Hiroshi Kiyono, Division of Mucosal Immunology, Department of Microbiology and Immunology, The Institute of Medical Science, The University of Tokyo, 4-6-1 Shirokanedai, Minato-ku, Tokyo 108-8639, Japan. E-mail address: kiyono@ims.u-tokyo.ac.jp

⁴ Abbreviations used in this paper: FAE, follicle-associated epithelium; 7-AAD, 7-amino actinomycin; CKLF, chemokine-like factor; CT, cholera toxin; DAPI, 4',6-diamidino-2-phenylindole; IEC, intestinal epithelial cell; IEL, intraepithelial lymphocyte; ISH, in situ hybridization; MLP, myristoylated alanine-rich C kinase substrate (MARCKS)-like protein; PP, Peyer's patch; UEA-1, *Ulex europaeus* agglutinin-1; WGA, wheat germ agglutinin.

Copyright © 2008 by The American Association of Immunologists, Inc. 0022-1767/08/\$2.00

www.jimmunol.org

Materials and Methods

Animals

BALB/c mice were purchased from Japan SLC. These mice were maintained under specific pathogen-free conditions in horizontal flow cabinets in our experimental animal facility at the University of Tokyo. Following a previously established protocol (9, 10), CT (List Biologic Laboratories) was dissolved in PBS (20 μ g/mouse) and then orally administered to BALB/c mice. Two days after CT administration, mice were used for experiments. All animal experiments were approved by the Animal Care and Use Committee of University of Tokyo.

Lectins and Abs for the detection of M cells

The following fluorescence-conjugated lectins and Abs were used for the identification of PP and villous M cells by FACS and histochemistry: PE-conjugated UEA-1 (Biogenesis), rhodamine-conjugated UEA-1 (Vector

Laboratories), biotin-conjugated UEA-1 (Vector Laboratories), FITC-conjugated wheat germ agglutinin (WGA) (Vector Laboratories), FITC-conjugated or biotin-conjugated M cell-specific NKM 16-2-4 mAb (8), and allophycocyanin-Cy7-conjugated anti-mouse CD45 mAb (30-F11; BD Biosciences).

Isolation of PP M cells, CT-induced villous M-like cells, and IECs

PPs from the naive duodenum and PP-free segments from the duodenum of naive or CT-administered mice were washed with cold PBS. Cells were dissociated from the small intestinal epithelium using a previously described mechanical procedure with some modifications (11). In brief, the tissues were incubated in PBS containing 0.5 mM EDTA with a stirrer for 10 min at 37°C. More than 90% of the dissociated cells survived as confirmed by a trypan blue exclusion test. The cells were stained with 1 μ g/ml FITC-conjugated NKM 16-2-4 mAb, 5 μ g/ml PE-conjugated UEA-1, and 1 μ g/ml allophycocyanin-Cy7-conjugated anti-mouse CD45 mAb for 40 min before being reacted with 7-amino actinomycin (7-AAD; BD Biosciences) diluted 1/5 in DMEM containing 10% FCS for 10 min on ice. After washing with DMEM containing 10% FCS, the stained cells were analyzed using a flow cytometer FACSaria (BD Biosciences), and suitable cell populations gated on CD45⁻ and 7-AAD⁻ cells were sorted.

DNA microarray analysis

Total RNA was extracted from the freshly isolated PP M cells, CT-induced villous M-like cells, and IECs of BALB/c mice using a High Pure RNA Tissue kit (Roche). Biotinylated cRNA was prepared using a two-cycle target-labeling assay in accordance with the protocol of the manufacturer (Affymetrix). The cRNA was hybridized with DNA probes on a GeneChip Mouse Genome 430 2.0 array (Affymetrix), washed, and fluorescence-labeled in accordance with the standard amplification protocol for eukaryotic targets developed by Affymetrix. The arrays were scanned with a GeneChip Scanner 3000 7G (Affymetrix). The fluorescence intensity of each probe was taken to represent the raw expression level and was quantified using GeneChip Operating software (Affymetrix). Data obtained from three independent experiments for PP M cells, CT-induced villous M-like cells, and IECs were normalized and statistically analyzed by Welch's ANOVA using GeneSpring 7.3.1 software (Silicon Genetics). In addition, both qualitative indices ("Present Call," "Marginal Call," and "Absent Call") based on *p*-value and a quantitative index (raw value) were also determined using GeneSpring 7.3.1 software. All microarray data described in this study have been deposited in the National Center for Biotechnology Information Gene Expression Omnibus database (www.ncbi.nlm.nih.gov/geo/) with the accession no. GSE7838.

In situ hybridization (ISH)

DNA fragments encoding GP2 (GenBank: NM_025989) and myristoylated alanine-rich C kinase substrate (MARCKS)-like protein (MLP; GenBank: NM_010807) were amplified by PCR from PP FAE-derived cDNA. The following sets of primers were used: *GP2*, sense, 5'-GGGTGATGGAGGAGTGAAGA-3', anti-sense, 5'-CTCCAGGATGTTCCACAGT-3'; and *MLP*, sense, 5'-AATTAACCCTCACTAAAGGGGAAGGCCAACGGACAGAGA-3', anti-sense, 5'-TAATACGACTCACTATAGGGCTTCTTGGGGGTCTCCTTGG-3' (T3 and T7 promoter sequences are shown by italics). The PCR products for GP2 were subcloned into a pCR4-TOPO vector (Invitrogen). After sequencing, digoxigenin-labeled sense and anti-sense RNA probes were transcribed in vitro from the subcloned plasmids or from T3 and T7 promoter-conjugated PCR products with DIG RNA labeling mix (Roche). Paraffin-embedded sections of small intestinal tissues (6 μ m) from naive BALB/c mice were obtained from Genostaff. ISH was performed as previously described (12). The bound probes were detected with BM purple AP substrate (Roche), before being counterstained with Kernechtrot stain solution (Muto Pure Chemicals) or reacted with 0.25 μ g/ml biotin-conjugated UEA-1 at 4°C overnight after treatment with 3% H₂O₂. The sections labeled with biotin-conjugated UEA-1 were further reacted with HRP-conjugated streptavidin, followed by staining with 3,3' diaminobenzidine (Vector Laboratories).

Generation of GP2- and MLP-specific Abs

For the generation of GP2- and MLP-specific Abs, the open reading frames of *GP2* and *MLP* genes were amplified by PCR from PP FAE-derived cDNA. The following sets of primers were used: *GP2*, sense, 5'-GACA TGCTAGCATGAAAAGGATGGTGGGTTGTGAC-3', anti-sense, 5'-GT ATCGAATTCTCAGAACAGTAGAGCCAGGAAGAC-3'; and *MLP*, sense, 5'-TGACTGAATTCATGGGACGCCAGAGCTCTAAGGCT-3', anti-sense, 5'-TACATGTGCACCTACTCATCTGCTCAGCACTGGC-3',

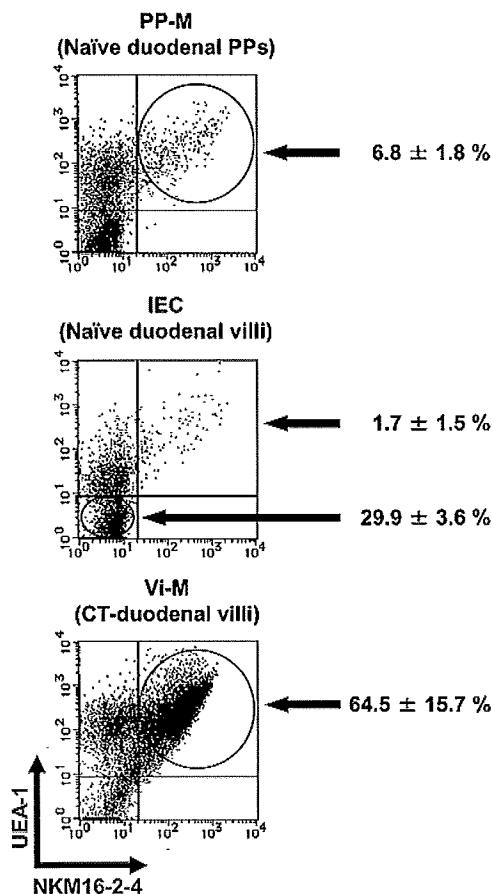


FIGURE 1. Frequency of PP M cells (PP-M) and CT-induced villous M-like cells (Vi-M) in the duodenal epithelium. Dot plots are shown by NKM 16-2-4-FITC and UEA-1-PE staining gated on CD45⁻ and 7-AAD⁻ duodenal epithelial cell populations from naive BALB/c mice or from those that had been orally treated with CT. PP-M (NKM 16-2-4⁺ and UEA-1⁺), Vi-M (NKM 16-2-4⁺ and UEA-1⁺), and IEC (NKM 16-2-4⁻ and UEA-1⁻) were isolated by FACS. Numbers are the mean percentage \pm SD in CD45⁻ and 7-AAD⁻ epithelial cell populations from three independent experiments.

[*NheI* and *EcoRI* (*GP2*), and *EcoRI* and *Sall* (*MLP*) restriction enzyme sites are shown by italics]. For generation of GP2-specific mAbs, amplified *GP2* gene was subcloned into pIRES2-EGFP vector (BD Biosciences) and the plasmid (pIRES2-GP2-EGFP) was then introduced in rat IEC line IEC-6 (ATCC, CRL-1592). After 2 days of transformation, EGFP-positive cells were purified by FACSaria and injected into the footpads of SD rats (1×10^6 cells/rat) five times at 2-wk intervals with TiterMax Gold (TiterMax) as an adjuvant. Four days after the final immunization, lymphocytes isolated from inguinal lymph node of the immunized rats were fused with P3 \times 63-AG8.653 myeloma cells (ATCC, CRL-1580) in the presence of 50% (w/v) polyethylene glycol 1500 (Roche). Established hybridomas were injected into Crlj; CD1-*Foxn1*tm mice and mAbs were purified from ascites by using Protein G-Sepharose (GE Healthcare). For generation of MLP-specific polyclonal Abs, the amplified *MLP* gene was subcloned into pGEX-4T-1 (GE Healthcare) and the plasmid (pMLP-GEX-4T-1) was then introduced in *Escherichia coli* DH5 α . After induction of MLP expression with 0.1 mM isopropyl β -D-thiogalactoside, the GST-fused MLP was purified on a Glutathione-Sepharose 4B (GE Healthcare) and subsequently removed the GST-tag with thrombin (GE Healthcare). The purified rMLP was then immunized into New Zealand white rabbits and anti-MLP pAbs were purified from the antiserum by using rMLP-conjugated TOYOPEARL AF-Tresyl-650M (Tosoh).

Histochemical analysis

The histochemical analyses were performed with whole-mount tissues and frozen-section specimens prepared from mucus-free tissues fixed with 4% paraformaldehyde in PBS as previously described (3). For GP2 staining,

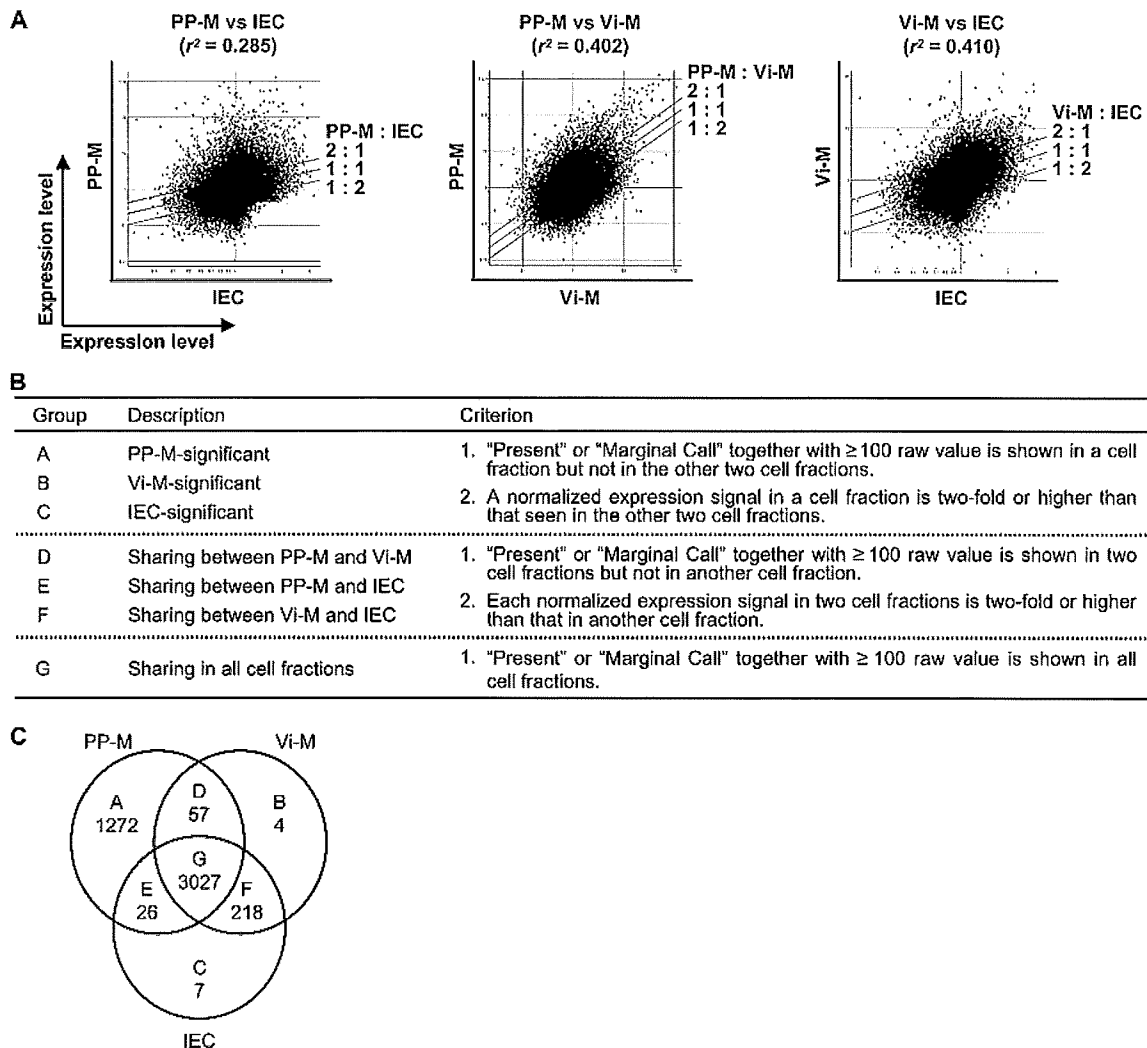


FIGURE 2. Gene expression profiles for PP M cells (PP-M), CT-induced villous M-like cells (Vi-M), and IECs. *A*, Scatter plots of the normalized expression level on each DNA microarray probe for PP-M and IEC, PP-M and Vi-M, and Vi-M and IEC with correlation coefficients (r^2). *B*, Grouping of probes based on their significance for PP-M, Vi-M, and IEC using the criteria outlined in the qualitative ("Present Call" or "Marginal Call") and quantitative (raw value) indices as assessed by GeneSpring 7.3.1 software. *C*, Venn diagram showing the categorization of significant probes into seven groups (Group A–G).

the specimens were incubated with 1 $\mu\text{g/ml}$ rat anti-GP2 mAb (10F5-9-2) or the isotype control Ab (rat IgG2a; BD Biosciences) at 4°C overnight. For MLP staining, tissue sections were incubated with 10 $\mu\text{g/ml}$ anti-MLP pAb or normal rabbit IgG at 4°C overnight. The specimens were then treated with 3 $\mu\text{g/ml}$ Cy5-conjugated donkey anti-rat IgG or 3 $\mu\text{g/ml}$ Cy5-conjugated donkey anti-rabbit IgG (Jackson ImmunoResearch Laboratories) together with 10 $\mu\text{g/ml}$ tetramethylrhodamine isothiocyanate-conjugated UEA-1 (Vector Laboratories) and/or 5 $\mu\text{g/ml}$ FITC-conjugated WGA (Vector Laboratories) for 1 h at room temperature. Finally, the section specimens were reacted with 400 ng/ml 4'-6-diamidino-2-phenylindole (DAPI; Sigma-Aldrich) and the signal was observed under a confocal laser-scanning microscope (TCS SP2; Leica). For counterstaining with our recently established M cell-specific mAb (NKM 16-2-4; rat IgG2c), the same section specimens were incubated with 5 $\mu\text{g/ml}$ biotin-conjugated NKM 16-2-4 at 4°C overnight followed by 1.25 $\mu\text{g/ml}$ HRP-conjugated streptavidin (Pierce) for 1 h at room temperature. The signal was then developed with 3,3'-diaminobenzidine and the nucleus was finally stained with hematoxylin.

Results

Isolation of PP M cells, CT-induced villous M-like cells, and IECs by FACS

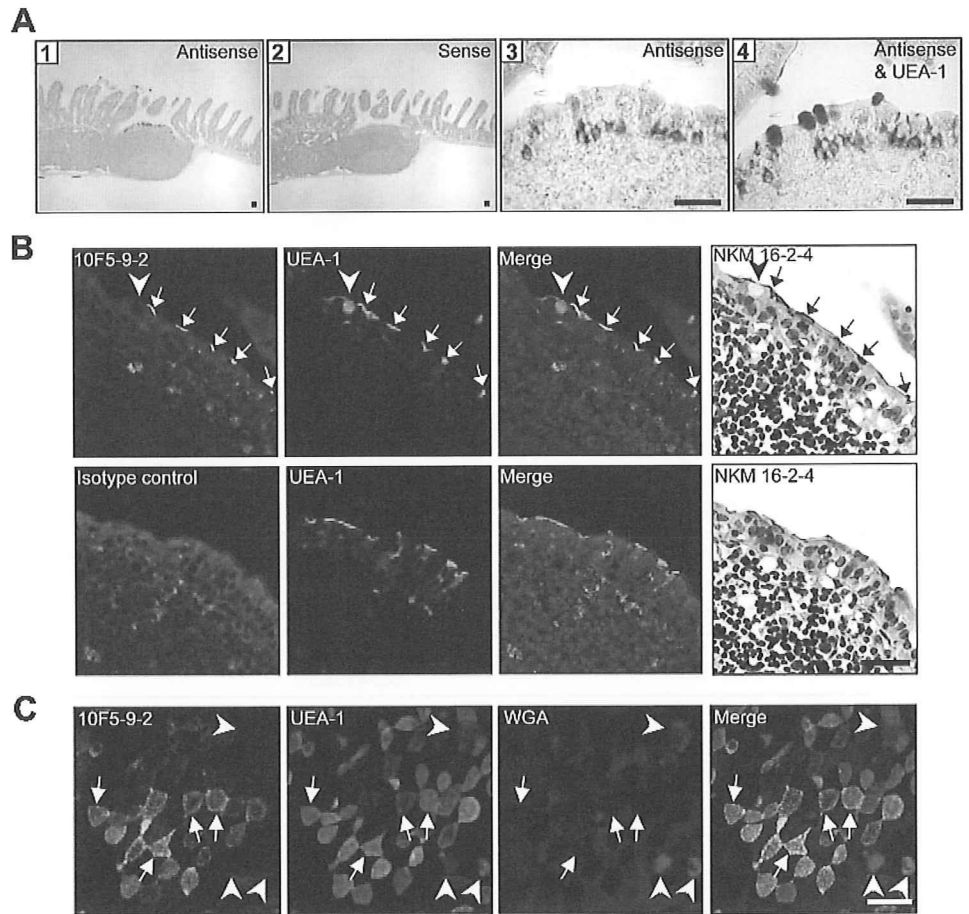
FACS analysis demonstrated that the large forward-scatter CD45⁺ cell population could be divided into three subpopulations by NKM 16-2-4 mAb and UEA-1 staining (Fig. 1). Because of the

known specificities of NKM 16-2-4 mAb and UEA-1, cells positive for NKM 16-2-4 and UEA-1 were identified as M cells (or M-like cells) in this study. In the CD45⁺ epithelial cell population isolated from the duodenum of naive BALB/c mice, the frequency of PP M cells averaged 7%. Perhaps due to the nature of the isolation technique used, the harvest of PP M cells far outstripped that of villous M cells, the frequency of the latter being so low ($1.7 \pm 1.5\%$) as to render harvest extremely difficult. We recently found that the number of villous M-like cells could be increased by oral administration of CT ($64.5 \pm 15.7\%$ and Terahara et al., submitted for publication), and so decided to use the villous M-like cells induced by CT treatment for this DNA microarray analysis. A FACS with a purity of 90–99% was used to isolate PP M cells (NKM 16-2-4⁺/UEA-1⁺), CT-induced villous M-like cells (NKM 16-2-4⁺/UEA-1⁺), and IECs (NKM 16-2-4⁻/UEA-1⁻).

Assessment of gene expression profiling of PP M cells, CT-induced villous M-like cells, and IECs

DNA microarrays containing 45,101 probes were used to determine the comprehensive gene expression of PP M cells, CT-induced villous M-like cells, and IECs. Comparison of these

FIGURE 3. GP2 was specifically expressed by PP M cells in the small intestine. **A**, ISH for GP2 mRNA with positive signals (blue) of hybridized anti-sense or sense cRNA probes on duodenal PPs and adjacent villi of naive BALB/c mice. Tissues were also counterstained with Kernechtrot (pink, 1 and 2) or labeled with UEA-1-HRP before being stained with 3,3'-diaminobenzidine (brown, 3 and 4). High magnification of a PP FAE before (3) and after (4) labeling with UEA-1. Scale bar = 200 μ m (1 and 2) and 40 μ m (3 and 4). **B**, Confocal images of frozen sections of PPs stained with anti-GP2-specific mAb (10F5-9-2) or isotype control (rat IgG2a). The specific expression of GP2 in M cells was confirmed by counterstaining with our recently established M cell-specific mAb (NKM 16-2-4). Arrows and arrowheads show M cells and goblet cells, respectively. Scale bar = 30 μ m. **C**, Confocal images of whole-mount duodenal PP domes stained with anti-GP2-specific mAb (10F5-9-2), UEA-1, and WGA. Scale bar = 30 μ m.



profiles revealed correlation coefficients of 0.285 for PP M cells and IECs, of 0.402 for PP M cells and CT-induced villous M-like cells, and of 0.410 for CT-induced villous M-like cells and IECs (Fig. 2A). Based on the constructed gene profiling, we categorized probes showing significant expression into seven groups (Groups A-G) using our own criteria (Fig. 2B). The 1272, 4, and 7 probes were regarded as significant for PP M cells (Group A), CT-induced villous M-like cells (Group B), and IECs (Group C), respectively (Fig. 2C). The relative expression levels and gene names of the significant probes are provided in Supplementary Table I.⁵ Our gene-profiling database allowed us to confirm previous findings that Group A includes the transcripts of peptidoglycan recognition protein-S, secretory granule neuroendocrine protein 1, and annexin V that are specifically expressed by PP M cells (4–6).

Specific expression of GP2 by PP M cells

In an effort to identify molecules that could be expressed on the apical surface of PP M cells, we looked for genes showing a higher expression level in Group A. During the ISH analysis, we found that GP2 mRNA was specifically expressed in the FAE of PPs throughout the small intestine (Fig. 3A, 1) and that its expression was distinctively colocalized with UEA-1⁺ M cells (Fig. 3A, 3 and 4). A negative control using sense cRNA probes did not show any positive signals (Fig. 3A, 2). Immunohistochemical analysis with newly established anti-GP2-specific mAb (10F5-9-2) revealed that the GP2 protein was highly expressed in UEA-1⁺ PP M cells (Fig. 3B). A negative control using isotype rat IgG2a did not show any

positive signals in the dome epithelium of PPs (Fig. 3B). The expression of GP2 in M cells was further confirmed by counterstaining with our recently established M cell-specific mAb NKM 16-2-4 (Fig. 3B). Supporting the histochemical analyses, whole-mount staining analysis also demonstrated GP2 was expressed on the apical surface of UEA-1⁺ PP M cells, which were not recognized by enterocyte-reactive lectin WGA (Fig. 3C). Supporting the gene profiling data (Supplementary Table I), GP2 protein was not detected in CT-induced villous M-like cells (data not shown).

Unique expression of MLP by PP M cells in the small intestine

Candidates for FAE-specific genes including *MLP* (also known as *MacMARCKS* or *MRP*) have been previously proposed (5, 6). Most of these genes together with *MLP* could be identified as PP M cell-significant genes by the DNA microarray analysis (Supplementary Table I). The subsequent ISH analysis demonstrated a unique expression pattern of *MLP* mRNA in the small intestine, i.e., *MLP* mRNA was detected in the FAE and B cell zones of PPs throughout the small intestine (Fig. 4A, 1). A negative control using sense cRNA probes did not show any positive signals (Fig. 4A, 2). In the FAE, the expression of *MLP* mRNA was exclusively colocalized with UEA-1⁺ M cells (Fig. 4A, 3 and 4). Immunohistochemical analysis further elucidated the complicated expression pattern of *MLP*, revealing that the *MLP* protein was also found in B cell zones and the cytoplasm of M cells in PPs throughout the small intestine (Fig. 4B), but not in CT-induced villous M-like cells (data not shown). A negative control using normal rabbit IgG did not show any positive signals (Fig. 4B).

⁵ The online version of this article contains supplemental material.

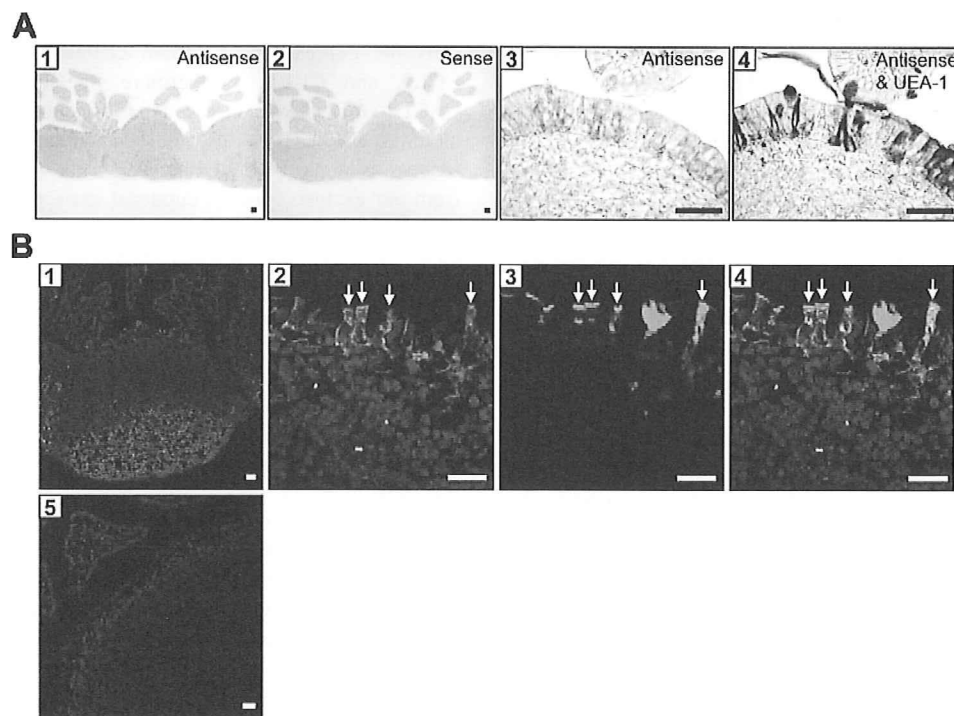


FIGURE 4. MLP was expressed by M cells and by the B cell zones of PPs but not by villi. *A*, ISH for MLP mRNA with positive signals (blue) of hybridized anti-sense or sense cRNA probes on duodenal PPs and adjacent villi of naive BALB/c mice. Tissues were also counterstained with Kernechtrot (pink, 1 and 2) or labeled with UEA-1-HRP before being stained with 3,3' diaminobenzidine (brown, 4). 3 and 4, High magnification of a PP FAE before (3) and after (4) labeling with UEA-1. Scale bar = 200 μ m (1 and 2) and 40 μ m (3 and 4). *B*, Confocal images of frozen sections of duodenal PPs from naive BALB/c mice labeled with UEA-1-rhodamine, DAPI, and immune complexes of FITC-labeled anti-rabbit IgG secondary Ab with anti-MLP polyclonal Ab or normal rabbit IgG. 1 and 5, Merged images of DAPI (blue) and MLP (green) (1) or normal rabbit IgG (green) (5). 2–4, High magnification of a PP FAE. 2, Merged image of DAPI (blue) and MLP (green)-staining. 3, Single image of UEA-1-staining (red). 4, Merged image of (2) and (3). Arrows show PP M cells expressing MLP. Scale bar = 100 μ m (1), 50 μ m (5), and 10 μ m (2–4).

Unique expression of chemokines in PP M cells and/or CT-induced villous M-like cells

Focusing on chemokines whose presence was statistically identified regardless of the raw value, we found seven chemokines to be expressed by PP M cells and/or CT-induced villous M-like cells (Table I). In addition to the previously reported CCL9 and CCL20 that are expressed by the M cell-containing PP FAE (13–15), we found significant expression of CXCL13 and chemokine-like factor (CKLF) in PP M cells. Although CT-induced villous M-like

cells and IECs constitutively expressed CCL6 and CCL28, the expression level of these chemokines was highest in PP M cells (thereby categorized in Group G; Fig. 2, B and C). Next, we also examined the expression pattern of chemokines in CT-induced villous M-like cells, finding, as in PP M cells, an up-regulation of CCL9, CKLF, and CCL6 mRNAs. Their raw values and expression levels were higher than those seen in IECs (Table I). Furthermore, CT-induced villous M-like cells showed the highest expression of CXCL16 mRNA, with expression levels 1.9–2.5-fold higher than in PP M cells and 2.1–2.3-fold higher than in IECs (Table I).

Table I. Chemokines expressed by PP M cells and/or CT-induced villous M-like cells^a

Name	GenBank	Affymetrix Probe No.	Group (see Fig. 2C)	Relative Expression Level against IEC	
				PP-M	Vi-M
CCL9	AF128196	1417936_at	A	124.8	7.0
CXCL13	AF030636	1417851_at	A	64.4	-
CKLF	BE852312	1436242_a_at	A	52.2	8.3
CCL6	AV084904	1420249_s_at	G	30.4	5.1
	BC002073	1417266_at	G	12.5	4.6
CCL20	AF099052	1422029_at	A	10.9	-
CCL28	BE196980	1455577_at	G	2.8	0.7
CXCL16	BC019961	1449195_s_at	G	1.1	2.1
		1418718_at	G	0.9	2.3

^a Expression levels on probes identified as "Present Call" in PP M cells (PP-M) or CT-induced villous M-like cells (Vi-M) were compared with those in IECs. Minus indicated no expression in Vi-M and IECs. CKLF, Chemokine-like factor.

Discussion

In this study, we combined the advanced techniques of M cell purification and DNA microarrays to construct a gene-profiling database for PP M cells, CT-induced villous M-like cells, and IECs. The lack of M cell-specific markers has long presented an obstacle to the isolation of M cells. We overcame this barrier by using M cell-specific NKM 16-2-4 mAb. Our knowledge that villous M (or M-like) cells, usually low frequency in the duodenum, could be increased by CT allowed us to separately isolate PP M cells, CT-induced villous M-like cells, and IECs using FACS. Of course, we cannot yet exclude the possibility that individual cell-sorted fractions were mildly contaminated by other cell types; however, we regard the database as reliable because most of the previously reported PP M cell-specific genes encoding peptidoglycan recognition protein-S, secretory granule neuroendocrine protein 1, and annexin V (4–6) were found in the PP M cell-significant group (Group A). Thus, the gene-profiling database presented

here has several advantages: it appears reliable because it was capable of confirming already established findings; it includes villous M (or M-like) cells as well as PP M cells and IECs; and it is based on a purified cell population. These advantages could make this gene-profiling database a reliable and useful tool for identifying new molecules expressed by M cells and for deepening our understanding of M cell immunobiology.

A mucosal vaccine delivery system targeting PP M cells would be more effective at generating not only efficient mucosal but also systemic immunity. When UEA-1 was used as an Ag delivery vehicle, the administration of PP M cell-targeted Ags induced Ag-specific mucosal and systemic immune responses (16) despite the cospecificity of the lectin for M cells and goblet cells (3). The gene-profiling database was, therefore, used to look for candidate target molecules in the vaccine delivery system. We focused on GP2, which is a GPI-anchored protein expressed at a higher level in Group A. GP2 is associated with lipid rafts, is sorted to the apical plasma membrane (17), and is likely to possess a similar distribution in PP M cells. Additional mRNA and protein analyses by ISH and immunohistochemistry identified the specific expression of GP2 in the apical plasma membrane of PP M cells. Although the role played by GP2 in a unique Ag-sampling system of PP M cells remains obscure, GP2 is not required for PP M cell development, as evidenced by the presence of M cells in the FAE of PPs from *GP2*^{-/-} mice (data not shown). Taken together, these findings support the candidacy of GP2 as an M cell-targeting molecule. If it is in fact confirmed to be so, it could greatly contribute to the development of a mucosal vaccine delivery system.

In addition to the identification of GP2, reliance of the gene-profiling database is further supported by the identification of specific expression of MLP by PP M cells. Not only *MLP* but also other genes have been previously reported as FAE-specific genes (5, 6). Using DNA microarray analysis, we were able to identify most such genes, including *MLP*, as PP M cell-significant genes. This study demonstrated for the first time the histological distribution of expressed MLP mRNA and protein in the small intestine. MLP, a member of protein kinase C substrates, binds calcium/calmodulin and actin (18, 19), and has been implicated in integrin-dependent phagocytosis by macrophages (20, 21). However, that contention was challenged in another study by Underhill and co-workers (22) using *MLP*^{-/-} macrophages. Interestingly, β 1 integrin, which is expressed by the apical membrane of PP M cells but not of IECs in the murine small intestine, is involved in the uptake of *Yersinia* by PP M cells via integrin-invasin binding (23). Thus, MLP may also account for the Ag uptake/sampling process, including integrin-dependent Ag uptake, of M cells located within the FAE of PPs.

Our constructed gene profiling also provides additional information for M cell immunobiology. Both PP and villous M cells contain in their basolateral region immunocompetent cells characterized by a pocket formation (3, 24), the contents of which are influenced by the repertoire of chemokines expressed by M cells. So far, three chemokines, CCL9, CCL20, and CXCL16, have been reported to be specifically expressed by the M cell-containing FAE of PPs and to contribute to the spatial distribution of dendritic cells or T cells in the subepithelial dome as well as in the basolateral pocket regions of M cells (13–15, 25). Our examination for the gene expression pattern of chemokines using the gene-profiling database showed that CXCL13, CKLF, CCL6, and CCL28, in addition to CCL9 and CCL20, are specifically or highly expressed by PP M cells, suggesting that CXCL13, CKLF, CCL6, and CCL28 may also play a role in regulating the recruitment of various immunocompetent cells into the pocket region of PP M cells.

Noticeably, CT-induced villous M-like cells share with PP M cells the expression of certain chemokines, including CCL6, CCL9, and CKLF. Furthermore, the highest expression of CXCL16 mRNA was observed in CT-induced villous M-like cells, although CXCL16 has previously been shown to be specifically expressed in the FAE of PPs (25). This discrepancy may result from our exclusive use of duodenal tissues for the analysis of M cell gene profiling. CXCL16 is a chemoattractant for activated CD8⁺ T cells and, to a lesser extent, for activated CD4⁺ T cells (25, 26); the CXCL16 receptor is expressed by intraepithelial lymphocytes (IELs) (26). In the small intestine, the distribution patterns for CD4⁺ and CD8⁺ T cells are distinct, with CD4⁺ T cells primarily located in the lamina propria and CD8⁺ T cells residing along the epithelium (27). When CT was orally administered, CD8⁺ IELs were rapidly and transiently depleted (28). Interestingly, we observed that CD8⁺ IEL numbers recovered following the generation of CT-induced villous M-like cells (data not shown). Therefore, our current finding that CT-induced villous M-like cells express a higher level of CXCL16 makes it plausible that CD8⁺ T cells are retained in the intestinal epithelium, mainly into the pocket of villous M-like cells. Furthermore, up-regulation of CCL9, CKLF, CCL6, and CXCL16 in CT-induced villous M-like cells could account for the CT-induced recruitment of immunocompetent cells to the site of Ag sampling from the intestinal lumen via CT-induced villous M-like cells.

Although the development mechanism of villous M cells remains unclear, we hypothesize that villous M cells are differentiated from IECs by exogenous stimuli because oral CT administration resulted in the induction of villous M-like cells in the middle to upper regions of villi (Terahara et al., submitted for publication), i.e., where IECs normally migrate from the crypts to the villus (29). Our hypothesis is also informed by the suggestions offered by other groups that IECs in the FAE of PPs could be converted to M cells by bacterial infection and inflammation (30, 31). We propose that CT-induced villous M-like cells have a gene expression pattern that is intermediate between PP M cells and IECs, as evidenced by the very similar correlation coefficient values obtained when the comprehensive gene profile of CT-induced villous M-like cells was compared with that of PP M cells ($r^2 = 0.402$) and IECs ($r^2 = 0.410$). The intermediate nature of CT-induced villous M-like cells between PP M cells and IECs is further confirmed by chemokine expression profiles. In this study, we have attempted to use gene profiling to elucidate the development mechanism of villous M cells.

In conclusion, our gene-profiling database should prove a valuable tool in identifying suitable M cell-targeting molecules, thereby speeding the development of a mucosal vaccine delivery system as well as allowing for a better understanding of M cell immunobiology.

Acknowledgments

We thank the members of our laboratory for technical advice and helpful discussions. We also extend our thanks to Dr. K. McGhee for editorial help.

Disclosures

The authors have no financial conflict of interest.

References

- Gebert, A., H. J. Rothkötter, and R. Pabst. 1996. M cells in Peyer's patches of the intestine. *Int. Rev. Cytol.* 167: 91–159.
- Neutra, M. R., A. Frey, and J. P. Kraehenbuhl. 1996. Epithelial M cells: gateways for mucosal infection and immunization. *Cell* 86: 345–348.
- Jang, M. H., M. N. Kweon, K. Iwatani, M. Yamamoto, K. Terahara, C. Sasakawa, T. Suzuki, T. Nochi, Y. Yokota, P. D. Rennert, et al. 2004. Intestinal villous M

- cells: an antigen entry site in the mucosal epithelium. *Proc. Natl. Acad. Sci. USA* 101: 6110–6115.
4. Lo, D., W. Tynan, J. Dickerson, J. Mendy, H. W. Chang, M. Scharf, D. Byrne, D. Brayden, L. Higgins, C. Evans, and D. J. O'Mahony. 2003. Peptidoglycan recognition protein expression in mouse Peyer's patch follicle associated epithelium suggests functional specialization. *Cell. Immunol.* 224: 8–16.
 5. Hase, K., S. Ohshima, K. Kawano, N. Hashimoto, K. Matsumoto, H. Saito, and H. Ohno. 2005. Distinct gene expression profiles characterized cellular phenotypes of follicle-associated epithelium and M cells. *DNA Res.* 12: 127–137.
 6. Verbrugge, P., W. Waelpu, B. Dieriks, A. Waeytens, J. Vandesompele, and C. A. Cuvelier. 2006. Murine M cells express annexin V specifically. *J. Pathol.* 209: 240–249.
 7. Clark, M. A., M. A. Jepson, N. L. Simmons, T. A. Booth, and B. H. Hirst. 1993. Differential expression of lectin-binding sites defines mouse intestinal M-cells. *J. Histochem. Cytochem.* 41: 1679–1687.
 8. Nochi, T., Y. Yuki, A. Matsumura, M. Mejima, K. Terahara, D. Y. Kim, S. Fukuyama, K. Iwatsuki-Horimoto, Y. Kawaoka, T. Kohda, et al. 2007. A novel M-cell-specific carbohydrate-targeted mucosal vaccine effectively induces antigen-specific immune responses. *J. Exp. Med.* 204: 2789–2796.
 9. Jackson, R. J., K. Fujihashi, J. Xu-Amano, H. Kiyono, C. O. Elson, and J. R. McGhee. 1993. Optimizing oral vaccines: induction of systemic and mucosal B-cell and antibody responses to tetanus toxoid by use of cholera toxin as an adjuvant. *Infect. Immun.* 61: 4272–4279.
 10. Xu-Amano, J., H. Kiyono, R. J. Jackson, H. F. Staats, K. Fujihashi, P. D. Burrows, C. O. Elson, S. Pillai, and J. R. McGhee. 1993. Helper T cell subsets for immunoglobulin A responses: oral immunization with tetanus toxoid and cholera toxin as adjuvant selectively induces Th2 cells in mucosa associated tissues. *J. Exp. Med.* 178: 1309–1320.
 11. Yamamoto, M., K. Fujihashi, K. Kawabata, J. R. McGhee, and H. Kiyono. 1998. A mucosal intranet: intestinal epithelial cells down-regulate intraepithelial, but not peripheral, T lymphocytes. *J. Immunol.* 160: 2188–2196.
 12. Yoshida, S., K. Ohbo, A. Takakura, H. Takebayashi, T. Okada, K. Abe, and Y. Nabeshima. 2001. Sgn1, a basic helix-loop-helix transcription factor delineates the salivary gland duct cell lineage in mice. *Dev. Biol.* 240: 517–530.
 13. Zhao, X., A. Sato, C. S. Dela Cruz, M. Linehan, A. Luegering, T. Kucharzik, A. K. Shirakawa, G. Marquez, J. M. Farber, I. Williams, and A. Iwasaki. 2003. CCL9 is secreted by the follicle-associated epithelium and recruits dome region Peyer's patch CD11b⁺ dendritic cells. *J. Immunol.* 171: 2797–2803.
 14. Iwasaki, A., and B. L. Kelsall. 2000. Localization of distinct Peyer's patch dendritic cell subsets and their recruitment by chemokines macrophage inflammatory protein (MIP)-3 α , MIP-3 β , and secondary lymphoid organ chemokine. *J. Exp. Med.* 191: 1381–1393.
 15. Cook, D. N., D. M. Prosser, R. Forster, J. Zhang, N. A. Kuklin, S. J. Abbondanzo, X. D. Niu, S. C. Chen, D. J. Manfra, M. T. Wiekowski, et al. 2000. CCR6 mediates dendritic cell localization, lymphocyte homeostasis, and immune responses in mucosal tissue. *Immunity* 12: 495–503.
 16. Wang, X., I. Kochetkova, A. Haddad, T. Hoyt, D. M. Hone, and D. W. Pascual. 2005. Transgene vaccination using *Ulex europaeus* agglutinin I (UEA-1) for targeted mucosal immunization against HIV-1 envelope. *Vaccine* 23: 3836–3842.
 17. Mays, R. W., K. A. Siemers, B. A. Fritz, A. W. Lowe, G. van Meer, and W. J. Nelson. 1995. Hierarchy of mechanisms involved in generating Na/K-ATPase polarity in MDCK epithelial cells. *J. Cell Biol.* 130: 1105–1115.
 18. Aderem, A. 1992. The MARCKS brothers: a family of protein kinase C substrates. *Cell* 71: 713–716.
 19. Blackshear, P. J. 1993. The MARCKS family of cellular protein kinase C substrates. *J. Biol. Chem.* 268: 1501–1504.
 20. Zhu, Z., Z. Bao, and J. Li. 1995. MacMARCKS mutation blocks macrophage phagocytosis of zymosan. *J. Biol. Chem.* 270: 17652–17655.
 21. Li, J., Z. Zhu, and Z. Bao. 1996. Role of MacMARCKS in integrin-dependent macrophage spreading and tyrosine phosphorylation of paxillin. *J. Biol. Chem.* 271: 12985–12990.
 22. Underhill, D. M., J. Chen, L. A. H. Allen, and A. Aderem. 1998. MacMARCKS is not essential for phagocytosis in macrophages. *J. Biol. Chem.* 273: 33619–33623.
 23. Clark, M. A., B. H. Hirst, and M. A. Jepson. 1998. M-cell surface β 1 integrin expression and invasin-mediated targeting of *Yersinia pseudotuberculosis* to mouse Peyer's patch M cells. *Infect. Immun.* 66: 1237–1243.
 24. Owen, R. L., and A. L. Jones. 1974. Epithelial cell specialization within human Peyer's patches: an ultrastructural study of intestinal lymphoid follicles. *Gastroenterology* 66: 189–203.
 25. Hase, K., T. Murakami, H. Takatsu, T. Shimaoka, M. Iimura, K. Hamura, K. Kawano, S. Ohshima, R. Chihara, K. Itoh, et al. 2006. The membrane-bound chemokine CXCL16 expressed on follicle-associated epithelium and M cells mediates lympho-epithelial interaction in GALT. *J. Immunol.* 176: 43–51.
 26. Matloubian, M., A. David, S. Engel, J. E. Ryan, and J. G. Cyster. 2000. A transmembrane CX chemokine is a ligand for HIV-coreceptor Bonzo. *Nat. Immunol.* 1: 298–304.
 27. Jahnsen, F. L., I. N. Farstad, J. P. Aanesen, and P. Brandtzaeg. 1998. Phenotypic distribution of T cells in human nasal mucosa differs from that in the gut. *Am. J. Respir. Cell Mol. Biol.* 18: 392–401.
 28. Flach, C. F., S. Lange, E. Jennische, I. Lönroth, and J. Holmgren. 2005. Cholera toxin induces a transient depletion of CD8⁺ intraepithelial lymphocytes in the rat small intestine as detected by microarray and immunohistochemistry. *Infect. Immun.* 73: 5595–5602.
 29. Leblond, C. P., and B. Messier. 1958. Renewal of chief cells and goblet cells in the small intestine as shown by radioautography after injection of thymidine-H3 into mice. *Anat. Rec.* 132: 247–259.
 30. Borghesi, C., M. J. Taussig, and C. Nicoletti. 1999. Rapid appearance of M cells after microbial challenge is restricted at the periphery of the follicle-associated epithelium of Peyer's patch. *Lab. Invest.* 79: 1393–1401.
 31. Lügering, A., M. Floer, N. Lügering, C. Cichon, M. A. Schmidt, W. Domschke, and T. Kucharzik. 2004. Characterization of M cell formation and associated mononuclear cells during indomethacin-induced intestinal inflammation. *Clin. Exp. Immunol.* 136: 232–238.

Regulation of humoral and cellular gut immunity by lamina propria dendritic cells expressing Toll-like receptor 5

Satoshi Uematsu^{1,2,12}, Kosuke Fujimoto^{1,2,12}, Myoung Ho Jang³, Bo-Gie Yang¹, Yun-Jae Jung⁴, Mika Nishiyama⁵, Shintaro Sato⁶, Tohru Tsujimura⁷, Masafumi Yamamoto⁸, Yoshifumi Yokota⁹, Hiroshi Kiyono⁶, Masayuki Miyasaka⁵, Ken J Ishii^{1,10,11} & Shizuo Akira^{1,2,10}

The intestinal cell types responsible for defense against pathogenic organisms remain incompletely characterized. Here we identify a subset of CD11c^{hi}CD11b^{hi} lamina propria dendritic cells (LPDCs) that expressed Toll-like receptor 5 (TLR5) in the small intestine. When stimulated by the TLR5 ligand flagellin, TLR5⁺ LPDCs induced the differentiation of naive B cells into immunoglobulin A–producing plasma cells by a mechanism independent of gut-associated lymphoid tissue. In addition, by a mechanism dependent on TLR5 stimulation, these LPDCs promoted the differentiation of antigen-specific interleukin 17–producing T helper cells and type 1 T helper cells. Unlike spleen DCs, the LPDCs specifically produced retinoic acid, which, in a dose-dependent way, supported the generation and retention of immunoglobulin A–producing cells in the lamina propria and positively regulated the differentiation of interleukin 17–producing T helper cells. Our findings demonstrate unique properties of LPDCs and the importance of TLR5 for adaptive immunity in the intestine.

The gastrointestinal tract is constantly exposed to food proteins and commensal bacteria. Although the intestinal immune system has evolved mechanisms to maintain immunological tolerance to food and commensal organisms, it also recognizes invasive pathogens and properly induces protective immune responses to eliminate them. Dendritic cells (DCs) are thought to be critical in the ‘decision’ of whether to mount tolerant or protective immune responses¹. Many subsets of DCs have been identified in the intestine². In the Peyer’s patches and mesenteric lymph nodes, conventional DCs consist of CD11c^{hi}CD11b⁺CD8 α ⁻, CD11c^{hi}CD11b⁻CD8 α ⁺ and CD11c^{hi}CD11b⁻CD8 α ⁻ subsets². In addition, there are CD11c^{int} plasmacytoid DCs in these sites^{3,4}. Peyer’s patch DCs produce interleukin 10 (IL-10) rather than IL-12, polarize naive T cells toward T helper type 2 (T_H2) or regulatory phenotypes⁵ and induce the differentiation of plasma cells positive for immunoglobulin A (IgA)^{6,7}.

In contrast, lamina propria DCs (LPDCs) are less well studied. Although DCs are dominant antigen-presenting cells in the small intestine, colonic DCs are concentrated mainly in isolated lymphoid

follicles, few of which are present in the lamina propria⁸. However, studies have shown that LPDCs of the small intestine and DCs in mesenteric lymph nodes that express CD103 have regulatory functions^{9,10}. CD103⁺ LPDCs migrate from the lamina propria to the mesenteric lymph nodes in a CCR7-dependent way^{11–13} and promote the generation of Foxp3⁺ regulatory T cells by means of retinoic acid¹⁴. Subsequent studies, however, have shown that CD11b⁺F4/80⁺CD11c⁻ macrophages in the lamina propria are more potent inducers of regulatory T cells than are LPDCs and that CD11b⁺ LPDCs generate T cells producing IL-17 *in vitro*¹⁵. These findings collectively suggest that LPDCs induce both ‘tolerogenic’ regulatory T cells and ‘inflammatory’ IL-17–producing T helper cells (T_H-17 cells). However, it remains unclear what kind of stimulation triggers the LPDC-induced generation of T_H-17 cells.

The Toll-like receptor (TLR) family, which is key for innate immunity, consists of 13 mammalian members¹⁶. TLRs are ‘preferentially’ expressed in ‘professional’ antigen-presenting cells such as DCs and macrophages and recognize specific components of

¹Laboratory of Host Defense, Immunology Frontier Research Center, Osaka University, 3-1 Yamada-oka, Suita, Osaka 565-0871, Japan. ²Department of Host Defense, Research Institute for Microbial Diseases, Osaka University, 3-1 Yamada-oka, Suita, Osaka 565-0871, Japan. ³Laboratory of Gastrointestinal Immunology, Immunology Frontier Research Center, Osaka University, Suita, Osaka 565-0871, Japan. ⁴Department of Microbiology, Gachon Medical School, Incheon 405-760, Korea. ⁵Laboratory of Immunodynamics, Department of Microbiology and Immunology, Osaka University Graduate School of Medicine, Osaka 565-0871, Japan. ⁶Division of Mucosal Immunology, Department of Microbiology and Immunology, The Institute of Medical Science, University of Tokyo, 108-8639 Tokyo, Japan. ⁷Department of Pathology, Hyogo College of Medicine, 1, Mukogawa, Nishinomiya, Hyogo 663-8501, Japan. ⁸Department of Microbiology and Immunology, Nihon University School of Dentistry at Matsudo, Chiba 271-8587, Japan. ⁹Division of Molecular Genetics, School of Medicine, Faculty of Medical Sciences, University of Fukui, Fukui 910-1193, Japan. ¹⁰Exploratory Research for Advanced Technology, Japan Science and Technology Corporation, 3-1 Yamada-oka, Suita, Osaka 565-0871, Japan. ¹¹Department of Molecular Protozoology, Research Institute for Microbial Diseases, Osaka University, 3-1 Yamada-oka, Suita, Osaka 565-0871, Japan. ¹²These authors contributed equally to this work. Correspondence should be addressed to S.A. (sakira@biken.osaka-u.ac.jp).

Received 26 March; accepted 5 May; published online 30 May 2008; doi:10.1038/ni.1622



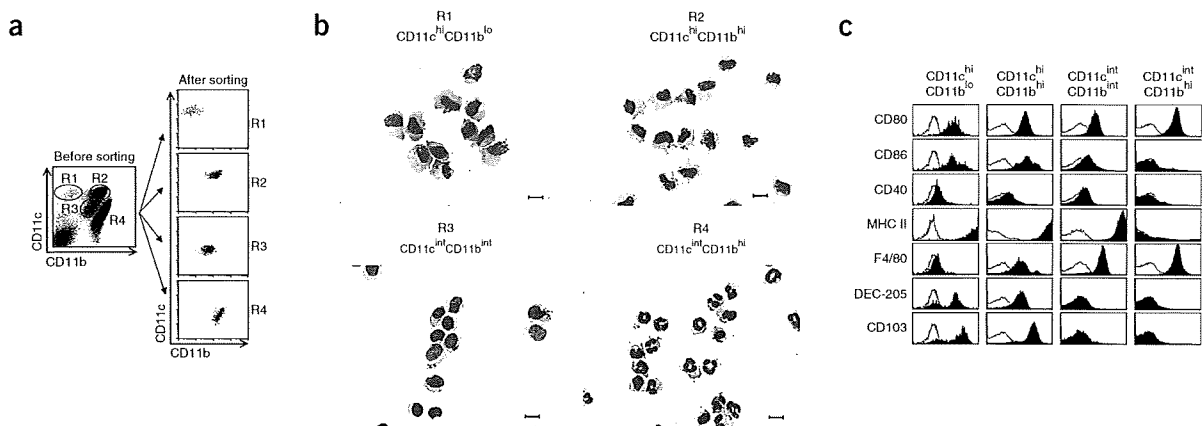


Figure 1 Four subsets of CD11c⁺ LPCs in the small intestine. (a) Flow cytometry of intestinal low-density LPCs stained for CD11b and CD11c, before and after sorting. (b) May-Grunwald-Giemsa staining of four leukocyte subsets (gated in a) from the lamina propria. Scale bars, 10 μ m. (c) Surface expression of CD80, CD86, CD40, major histocompatibility complex class II (MHC II), F4/80, DEC-205 and CD103 (filled histograms) on the four leukocyte subsets gated in a. Open histograms, isotype control. Data are representative of at least three independent experiments.

microorganisms to induce innate immune responses¹⁶. Each TLR activates specific signaling pathways that elicit biological responses to microorganisms, as well as DC maturation and cytokine production that shape adaptive immune responses¹⁶. Although the function of TLRs has been examined extensively in intestinal epithelial cells¹⁷, the function of TLRs in lamina propria antigen-presenting cells has not been fully elucidated. Intestinal CD11c⁺ lamina propria cells (LPCs) have high expression of TLR5 (A002297) and induce inflammatory responses when stimulated with the TLR5 ligand bacterial flagellin¹⁸. Unlike conventional DCs, such as those in the spleen (SPDCs), CD11c⁺ LPCs do not express TLR4, which recognizes the Gram-negative bacterial component lipopolysaccharide (LPS)¹⁸. Nevertheless, *Thr5*^{-/-} mice show resistance to oral *Salmonella typhimurium* infection, as this facultative intracellular flagellated bacteria seems to use TLR5 and CD11c⁺ LPCs as 'carriers' for systemic infection¹⁸.

Mouse CD11c⁺ LPCs consist of four subsets distinguished by differential expression patterns of CD11c and CD11b. Here we have identified a subset of CD11c^{hi}CD11b^{hi} LPDCs as TLR5-expressing cells. In response to flagellin, these LPDCs induced the differentiation of naive B cells into IgA⁺ (A001174) plasma cells by a mechanism independent of gut-associated lymphoid tissue (GALT) and triggered the differentiation of antigen-specific T_H-17 and T_H1 cells. In a dose-dependent way, retinoic acid produced by LPDCs supported the generation and retention of IgA-producing cells in the lamina propria and positively regulated T_H-17 cell differentiation.

RESULTS

High TLR5 expression on CD11c^{hi}CD11b^{hi} LPDCs

CD11c⁺ DCs constituted 10–15% of leukocytes in the small intestinal lamina propria and consisted of at least two subsets (CD11c^{hi}CD11b^{lo} (R1) and CD11c^{hi}CD11b^{hi} (R2))¹² (Fig. 1a,b), each of which had a DEC-205⁺ major histocompatibility complex class II–high CD80⁺CD86⁺CD103⁺ surface phenotype (Fig. 1c). In addition, CD11c^{hi}CD11b^{hi} cells had moderate expression of F4/80, which indicated a macrophage-like character. The remaining CD11c⁺ subsets consisted of CD11c^{int}CD11b^{int} cells (R3), which are F4/80⁺DEC-205⁻ major histocompatibility complex class II⁺ phagocytic macrophages^{15,19}, and CD11c^{int}CD11b^{hi} cells (R4), which are eosinophils

with uniquely shaped nuclei and eosinophilic granules¹² (Fig. 1b,c). Of these four subsets from the lamina propria of C57BL/6 mice, only CD11c^{hi}CD11b^{hi} LPDCs expressed *Thr5* mRNA (Fig. 2a). Consistent with the expression of functional TLR5, CD11c^{hi}CD11b^{hi} LPDCs produced proinflammatory cytokines such as IL-6, IL-12p40 and IL-12p70, but not IL-23 or IL-10, in response to flagellin (Fig. 2b). In contrast, LPDCs (R1) did not produce such cytokines in response to either flagellin or LPS (Supplementary Fig. 1 online). Thus, CD11c^{hi}CD11b^{hi} LPDCs are responsible for TLR5-mediated innate immune responses.

CD11c^{hi}CD11b^{hi} LPDCs induce IgA production

To determine the function of CD11c^{hi}CD11b^{hi} LPDCs in adaptive immunity, we examined IgA synthesis in the small intestine. IgA is the

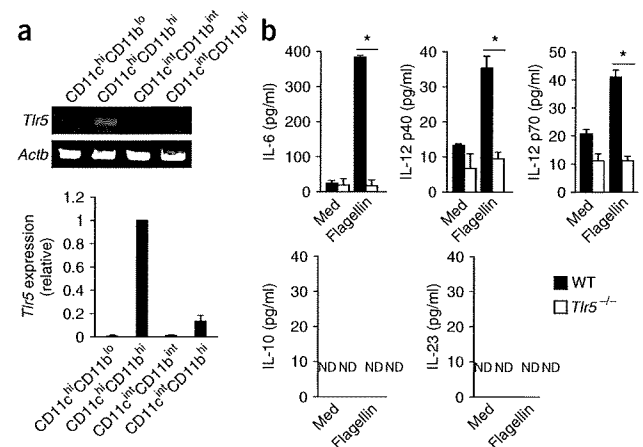


Figure 2 CD11c^{hi}CD11b^{hi} LPDCs specifically express TLR5. (a) RT-PCR (top) and quantitative real-time PCR (bottom) of *Thr5* expression in the four leukocyte lamina propria subsets. *Actb* encodes β -actin (top, loading control). Expression (bottom) is relative to that of *Actb*. Data are representative of three independent experiments. (b) Cytokine production by CD11c^{hi}CD11b^{hi} LPDCs from wild-type (WT) and *Thr5*^{-/-} mice in response to medium alone (Med) or flagellin (1 μ g/ml). ND, not detected. *, $P < 0.05$ (unpaired Student's *t*-test). Data represent the mean and s.d. of three independent experiments.



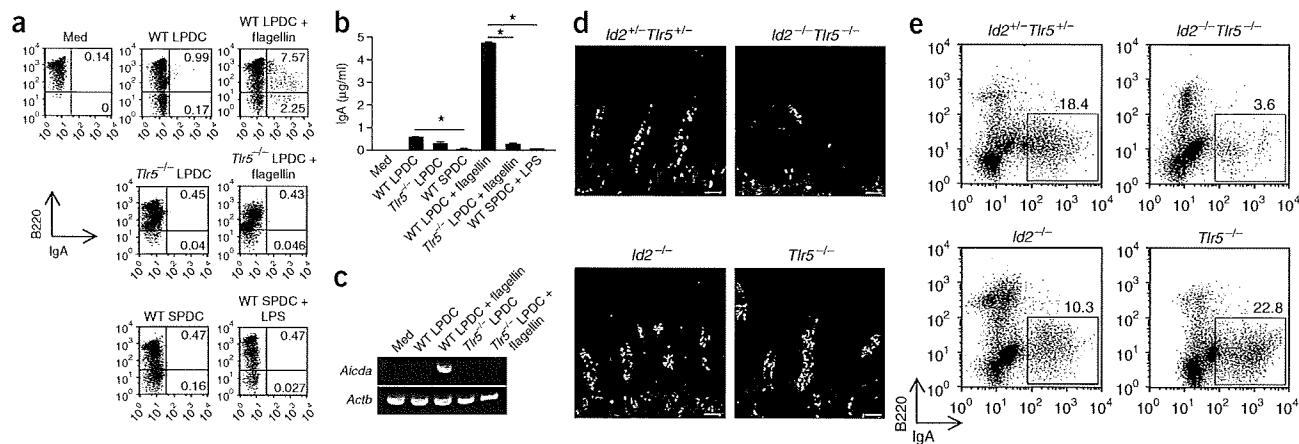


Figure 3 CD11c^{hi}CD11b^{hi} LPDCs induce IgA⁺ plasma cell differentiation. (a,b) Flow cytometry (a) and ELISA (b) of peritoneal IgM⁺IgD⁺ cells cultured for 5 d in various conditions (above plots (a) and below horizontal axis (b)). (a) Cells stained for B220 and IgA (isotype controls, **Supplementary Fig. 2**). Numbers in quadrants indicate percent B220⁺IgA⁺ cells (top right) or B220⁻IgA⁺ cells (bottom right). Data are representative of three independent experiments. (b) Concentration of IgA in coculture supernatants. *, $P < 0.05$ (unpaired Student's *t*-test). Data represent the mean and s.d. of three independent experiments. (c) Expression of *Aicda* mRNA (encoding activation-induced cytidine deaminase) in IgM⁺IgD⁺ cells cultured together with wild-type or *Tlr5*^{-/-} CD11c^{hi}CD11b^{hi} LPDCs with or without flagellin. Data are representative of three independent experiments. (d) Immunohistochemistry of IgA⁺ cells (green) in the small intestine ($n = 4$ mice per group). Scale bars, 50 μ m. Data are representative of three independent experiments. (e) Flow cytometry of LPCs stained for B220 and IgA. Numbers above outlined areas indicate percent B220⁻IgA⁺ cells. Data are representative of three independent experiments.

most abundant immunoglobulin in the gut²⁰. Intestinal IgA⁺ plasma cells are generated mainly in GALT, including Peyer's patches, isolated lymphoid follicles and mesenteric lymph nodes, by a mechanism dependent on antigen, T cells and the formation of germinal centers^{21–23}. Differentiated IgA⁺ cells are 'imprinted' by GALT DC-derived retinoic acid for gut homing through the selective expression of gut-homing receptors, including integrin $\alpha_4\beta_7$ and CCR9 (ref. 7). However, reports have shown that IgA⁺ cell development does not necessarily require T cell help and the formation of germinal centers^{21,24} and that GALT DC-derived retinoic acid can potentially act in synergy with cytokines produced by DCs and/or other cells to generate T cell-independent IgA⁺ cells⁷. Furthermore, it seems that some IgM⁺ B cells, especially peritoneal B1 cells, migrate directly to the gut lamina propria by

a mechanism dependent on sphingosine 1-phosphate^{25,26} and differentiate into IgA⁺ plasma cells in the lamina propria with the help of stroma cells²⁴. Commensal bacteria induce natural secretory IgA, and this process is mediated by DCs loaded with commensal bacteria^{6,27}. Nevertheless, although published work has suggested the involvement of DCs in gut IgA production^{28,29}, it is unknown what subset of DCs is responsible for this event and how this is achieved. We thus examined whether CD11c^{hi}CD11b^{hi} LPDCs are involved in the generation of IgA⁺ cells; we used SPDCs (TLR5-TLR4⁺) for comparison¹⁸. Flagellin-stimulated CD11c^{hi}CD11b^{hi} LPDCs but not LPS-stimulated SPDCs efficiently induced the differentiation of B220⁻IgA⁺ plasma cells in the absence of T cells in a TLR5-dependent way (Fig. 3a,b and **Supplementary Fig. 2** online). Expression of

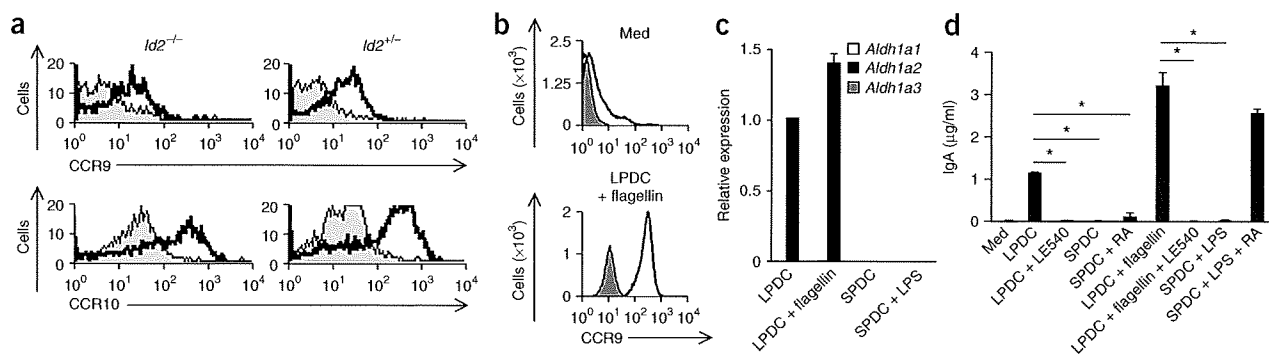


Figure 4 Function of retinoic acid released by CD11c^{hi}CD11b^{hi} LPDCs in IgA synthesis. (a) Flow cytometry of LPCs stained for B220, IgA, CCR9 or CCR10 (open histograms), gated on B220⁻IgA⁺ cells. Filled histograms, isotype control. Data are representative of three independent experiments. (b) Flow cytometry of peritoneal B220⁺ cells cultured for 5 d with or without flagellin-stimulated CD11c^{hi}CD11b^{hi} LPDCs. Data for CCR9 (open histograms) were acquired after gating on B220⁺ cells (top) or B220⁻IgA⁺ cells (bottom). Filled histograms, isotype control. Data are representative of three independent experiments. (c) Quantitative real-time PCR of mRNA encoding retinal dehydrogenase isozymes (key) in CD11c^{hi}CD11b^{hi} LPDCs and SPDCs left unstimulated or stimulated with LPS or flagellin (horizontal axis). Data are representative of three independent experiments (mean and s.d.). (d) ELISA of IgA in supernatants of peritoneal B220⁺ cells cultured for 5 d in various conditions (horizontal axis) with or without LE540 (1 μ M) or retinoic acid (RA; 1 nM). *, $P < 0.05$ (unpaired Student's *t*-test). Data represent the mean and s.d. of three independent experiments.

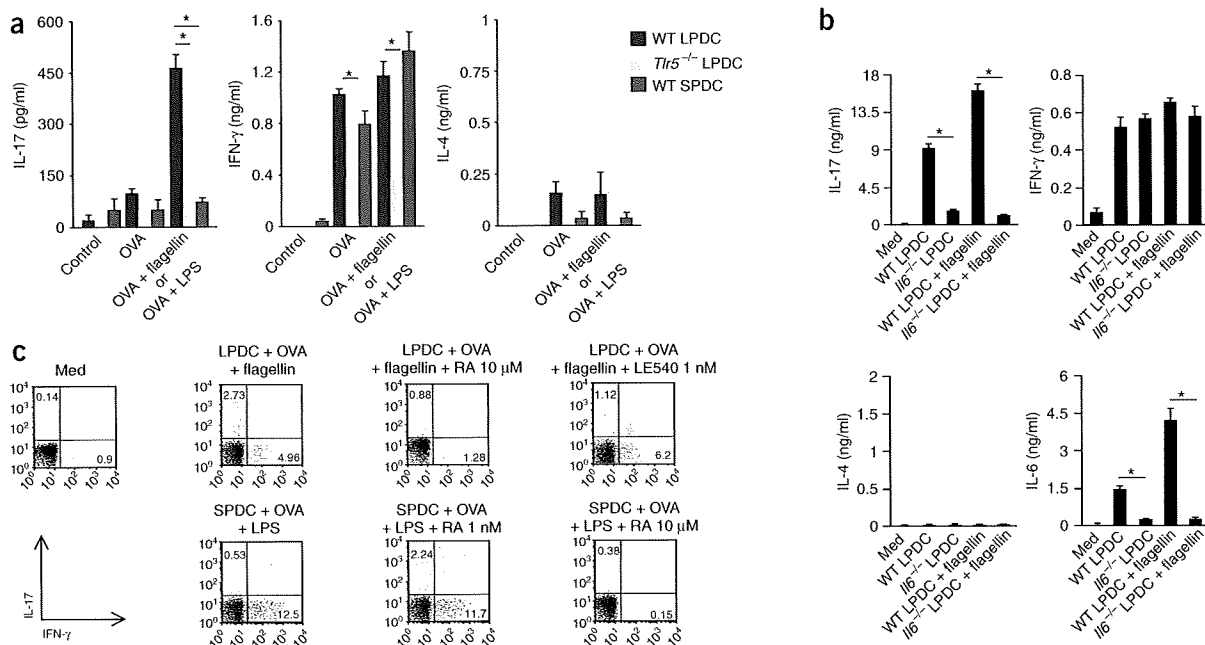


Figure 5 TLR5-dependent T_H -17 cell differentiation by $CD11c^{hi}CD11b^{hi}$ LPDCs. (a) ELISA of IFN- γ , IL-17 and IL-4 in culture supernatants. $CD11c^{hi}CD11b^{hi}$ LPDCs or SPDCs cultured for 12 h with OVA protein (100 μ g/ml) in the presence or absence of flagellin (1 μ g/ml) or LPS (1 μ g/ml) were injected on days 0 and 14 into the peritoneal cavities of naive *Tlr5*^{-/-} mice (wild-type $CD11c^{hi}CD11b^{hi}$ LPDCs) or *Tlr4*^{-/-} mice (wild-type SPDCs) at a dose of 5×10^4 antigen-loaded cells per mouse; control mice were treated with PBS. At 1 week after the final immunization, splenocytes were collected and were cultured for 4 d with OVA protein (10 μ g/ml) or with OVA peptide (amino acids 323–339; 10 μ g/ml; **Supplementary Fig. 6**). *, $P < 0.05$ (unpaired Student's *t*-test). Data represent the mean and s.d. of three independent experiments. (b) ELISA of cytokines in supernatants of OT-II transgenic $CD4^+$ T cells cultured for 4 d together with wild-type or *Il6*^{-/-} $CD11c^{hi}CD11b^{hi}$ LPDCs (conditions, horizontal axes). *, $P < 0.05$ (unpaired Student's *t*-test). Data represent the mean and s.d. of three independent experiments. (c) Flow cytometry of OT-II transgenic $CD4^+$ T cells cultured for 4 d in various conditions (above plots) and stained intracellularly for IL-17 and IFN- γ (isotype controls, **Supplementary Fig. 7a**). Numbers in quadrants indicate percent IL-17⁺IFN- γ ⁺ cells (top left) or IL-17⁺IFN- γ ⁻ cells (bottom right). Data are representative of three independent experiments.

mRNA encoding activation-induced cytidine deaminase³⁰, an enzyme essential for class-switch recombination, was upregulated in naive B cells cultured together with flagellin-stimulated $CD11c^{hi}CD11b^{hi}$ LPDCs (Fig. 3c).

Although the results presented above demonstrated that $CD11c^{hi}CD11b^{hi}$ LPDCs were able to induce T cell-independent differentiation of IgA^+ cells *in vitro*, we also examined the *in vivo* function of TLR5 in IgA synthesis by using GALT-deficient mice that intrinsically lack secondary lymphoid organs but have LPDCs. Mice lacking the transcription factors *Id2* or *ROR γ t*, as well as bone marrow-reconstituted mice lacking lymphotoxin- α or both lymphotoxin- α and tumor necrosis factor, do not develop GALT, yet they retain intestinal IgA production^{21,31}. Indeed, we detected many IgA^+ cells in the lamina propria of *Id2*^{-/-} mice, which confirmed that gut IgA can be generated without GALT (Fig. 3d,e). Furthermore, we found no defects in the *in vitro* differentiation of IgA^+ plasma cells induced by $CD11c^{hi}CD11b^{hi}$ LPDCs from peritoneal B cells isolated from *Id2*^{-/-} mice (**Supplementary Fig. 3** online). Although *Tlr5*^{-/-} mice did not have fewer IgA^+ B cells, *Id2*^{-/-}*Tlr5*^{-/-} mice had far fewer IgA^+ cells in the lamina propria (Fig. 3d,e). Thus, TLR5 signaling in $CD11c^{hi}CD11b^{hi}$ LPDCs is critical for GALT-independent IgA synthesis *in vivo*.

Retinoic acid in LPDC-induced IgA synthesis

We next examined the expression of gut-homing receptors on lamina propria IgA^+ cells in *Id2*^{-/-} mice. Unexpectedly, B220⁺ IgA^+ plasma cells in the lamina propria of *Id2*^{-/-} mice had high expression of CCR9, despite the lack of GALT in these mice (Fig. 4a). These cells also

expressed CCR10, another chemokine receptor important for gut tropism³². As we did not detect high CCR9 expression on either peritoneal or splenic unstimulated B220⁺ cells from wild-type or *Id2*^{-/-} mice (Fig. 4b and data not shown), CCR9 might be induced on B cells only after their migration to the lamina propria in *Id2*^{-/-} mice. In contrast, coculture with flagellin-treated $CD11c^{hi}CD11b^{hi}$ LPDCs induced CCR9 expression on peritoneal B220⁺ IgA^+ cells (Fig. 4b). We therefore determined whether $CD11c^{hi}CD11b^{hi}$ LPDCs synthesize retinoic acid, a mediator able to induce CCR9 expression. Retinal is converted into retinoic acid by retinal dehydrogenase enzymes. Although we detected no mRNA molecules encoding retinal dehydrogenase isoforms in SPDCs, $CD11c^{hi}CD11b^{hi}$ LPDCs specifically expressed *Aldh1a2* mRNA, which encodes retinal dehydrogenase 2 (Fig. 4c). To determine if the $CD11c^{hi}CD11b^{hi}$ LPDC-mediated development of IgA^+ cells was controlled by retinoic acid, we added the retinoic acid receptor inhibitor LE540 during the *in vitro* coculture of B cells and $CD11c^{hi}CD11b^{hi}$ LPDCs. LE540 abrogated IgA production by B cells cultured together with flagellin-activated $CD11c^{hi}CD11b^{hi}$ LPDCs (Fig. 4d). Moreover, supplementation of LPS-activated SPDCs with retinoic acid increased IgA concentrations to an extent similar to that induced by flagellin-activated $CD11c^{hi}CD11b^{hi}$ LPDCs. Thus, the characteristic ability to synthesize retinoic acid grants $CD11c^{hi}CD11b^{hi}$ LPDCs the ability to generate T cell-independent IgA^+ cells.

LPDC-induced T_H -17 cell differentiation

We next assessed the ability of $CD11c^{hi}CD11b^{hi}$ LPDCs to induce antigen-specific T helper cell differentiation of ovalbumin

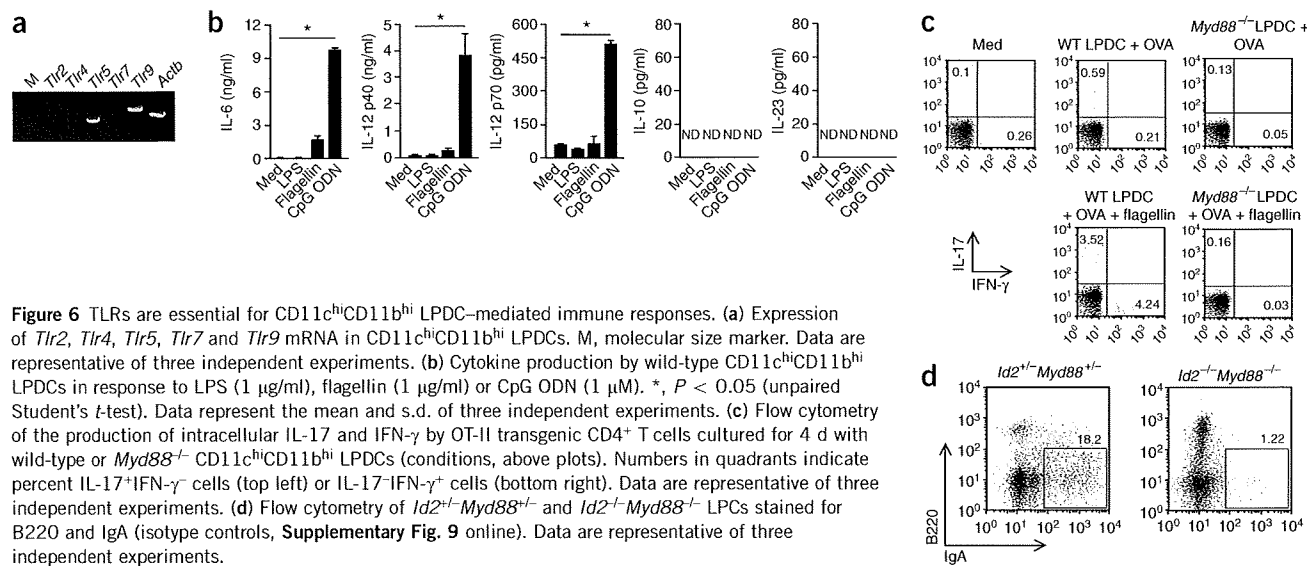


Figure 6 TLRs are essential for CD11c^{hi}CD11b^{hi} LPDC-mediated immune responses. (a) Expression of *Tlr2*, *Tlr4*, *Tlr5*, *Tlr7* and *Tlr9* mRNA in CD11c^{hi}CD11b^{hi} LPDCs. M, molecular size marker. Data are representative of three independent experiments. (b) Cytokine production by wild-type CD11c^{hi}CD11b^{hi} LPDCs in response to LPS (1 μg/ml), flagellin (1 μg/ml) or CpG ODN (1 μM). *, $P < 0.05$ (unpaired Student's *t*-test). Data represent the mean and s.d. of three independent experiments. (c) Flow cytometry of the production of intracellular IL-17 and IFN-γ by OT-II transgenic CD4⁺ T cells cultured for 4 d with wild-type or *Myd88*^{-/-} CD11c^{hi}CD11b^{hi} LPDCs (conditions, above plots). Numbers in quadrants indicate percent IL-17⁺IFN-γ⁻ cells (top left) or IL-17⁺IFN-γ⁺ cells (bottom right). Data are representative of three independent experiments. (d) Flow cytometry of *Id2*⁺*Myd88*⁺ and *Id2*⁻*Myd88*⁻ LPDCs stained for B220 and IgA (isotype controls, **Supplementary Fig. 9** online). Data are representative of three independent experiments.

(OVA)-specific OT-II-transgenic CD4⁺ T cells. Although we detected only interferon-γ (IFN-γ)-producing cells in cocultures of OT-II T cells and LPS-stimulated SPDCs, we detected both IL-17- and IFN-γ-producing cells in cocultures of OT-II T cells and CD11c^{hi}CD11b^{hi} LPDCs; the numbers of IL-17- and IFN-γ-producing OT-II cells were further increased by flagellin stimulation of LPDCs^{33–36} (**Supplementary Fig. 4a,b** online). In support of the idea that TLR5⁺ CD11c^{hi}CD11b^{hi} LPDCs induce T_H-17 differentiation, naive CD4⁺ T cells cultured together with wild-type CD11c^{hi}CD11b^{hi} LPDCs had higher expression of RORγt and IL-21, but those cultured together with *Tlr5*^{-/-} CD11c^{hi}CD11b^{hi} LPDCs did not (**Supplementary Fig. 4c,d**). In contrast, other LPDC subsets (R1, R3 and R4) induced neither IL-17 nor IFN-γ production in response to flagellin (**Supplementary Fig. 5** online).

Next we examined *in vivo* the T helper cell responses of mice immunized with antigen-loaded DCs. We detected antigen-specific IFN-γ production after injection of both SPDCs and CD11c^{hi}CD11b^{hi} LPDCs, and this production was augmented by stimulation of TLR5 and TLR4 (**Fig. 5a** and **Supplementary Fig. 6** online). In addition, large amounts of IL-17 were produced by splenocytes from mice injected with flagellin-stimulated CD11c^{hi}CD11b^{hi} LPDCs but not those injected with LPS-stimulated SPDCs. Those responses were impaired when mice were injected with *Tlr5*^{-/-} CD11c^{hi}CD11b^{hi} LPDCs. As IL-6 is an essential cytokine for T_H-17 cell differentiation, and as CD11c^{hi}CD11b^{hi} LPDCs produced IL-6 in response to TLR5 stimulation (**Fig. 2b**), we then examined the involvement of IL-6 in CD11c^{hi}CD11b^{hi} LPDCs-induced T_H-17 cell differentiation³⁷. Despite normal induction of IFN-γ, IL-17 production induced by flagellin-stimulated *Il6*^{-/-} CD11c^{hi}CD11b^{hi} LPDCs was significantly lower than that elicited by flagellin-stimulated wild-type CD11c^{hi}CD11b^{hi} LPDCs (**Fig. 5b**).

A series of studies has shown that retinoic acid negatively regulates T_H-17 cell differentiation^{38–40}. In agreement with those results, supplementation of cocultures of T cells and CD11c^{hi}CD11b^{hi} LPDCs with 10 μM retinoic acid effectively inhibited *in vitro* T_H-17 cell differentiation; retinoic acid supplementation also suppressed T_H1 cell differentiation (**Fig. 5c** and **Supplementary Fig. 7** online). However, we suspected that this concentration of retinoic acid may have been too high, as plasma retinoic acid concentrations are usually

on the order of 10 nM and retinoic acid efficiently enhances the expression of gut-homing receptors on CD8⁺ T cells even at a concentration of 0.1 nM (ref. 41). Notably, the retinoic acid inhibitor LE540 inhibited the differentiation of T_H-17 cells but not T_H1 cells, which suggested that retinoic acid from CD11c^{hi}CD11b^{hi} LPDCs is actually necessary for T_H-17 cell differentiation. In line with that observation, LPS-stimulated SPDCs induced T_H-17 cell differentiation to the same extent as flagellin-stimulated CD11c^{hi}CD11b^{hi} LPDCs when cultured together with 1 nM retinoic acid, and 10 μM retinoic acid abolished T_H1 cell differentiation induced by LPS-stimulated SPDCs (**Fig. 5c** and **Supplementary Fig. 7**). Thus, retinoic acid at a low concentration acts as a positive regulator of T_H-17 cell differentiation, and the effect of retinoic acid on T_H-17 cell differentiation depends on its concentration.

CD11c^{hi}CD11b^{hi} LPDCs induce antigen-specific T_H-17 cells and T_H1 cells, but it is not clear whether these adaptive immune responses are protective against bacterial infection. T_H-17 cells constitute approximately 2% of the total CD4⁺ T cell population in the small intestinal lamina propria of C57BL/6 mice without infection, and the number of T_H-17 cells did not change during the acute phase of oral *S. typhimurium* infection (**Supplementary Fig. 8a** online). Mice immunized with OVA-loaded CD11c^{hi}CD11b^{hi} LPDCs had greater proportions of T_H-17 and T_H1 cells in the lamina propria (**Supplementary Fig. 8b**). Challenge of the immunized mice with oral OVA further increased the proportions of lamina propria T_H-17 and T_H1 cells. Similarly, immunization with *S. typhimurium* flagellin-loaded wild-type LPDCs resulted in a significant increase in the proportion of lamina propria T_H-17 cells after oral challenge with *S. typhimurium*, ($P < 0.05$; **Supplementary Fig. 8c**) and resulted in partial protection against lethal challenge with *S. typhimurium* (**Supplementary Fig. 8d**), but similar immunization with *Tlr5*^{-/-} LPDCs did not. Thus, CD11c^{hi}CD11b^{hi} LPDC-mediated immunization contributed to host defense against *S. typhimurium*.

TLR signals in LPDC-mediated inflammation

Although we demonstrated the importance of TLR5 in the activation of adaptive immunity by CD11c^{hi}CD11b^{hi} LPDCs, *Tlr5*^{-/-} CD11c^{hi}CD11b^{hi} LPDCs nevertheless induced small amounts of IL-17- and IFN-γ-producing cells (**Supplementary Fig. 4a**). In



addition, we detected residual B220-IgA⁺ plasma cells in the lamina propria of *Id2*^{-/-}*Tlr5*^{-/-} mice (Fig. 3e). Thus, other TLRs may contribute to such responses. Accordingly, CD11c^{hi}CD11b^{hi} LPDCs expressed TLR9 as well as TLR5 and produced proinflammatory cytokines in response to the TLR9 ligand CpG DNA (Fig. 6a,b). Notably, unlike wild-type CD11c^{hi}CD11b^{hi} LPDCs, *Myd88*^{-/-} CD11c^{hi}CD11b^{hi} LPDCs failed to induce the *in vitro* differentiation of T_H-17 and T_H1 cells (Fig. 6c). Furthermore, B220-IgA⁺ cells were almost completely absent from the lamina propria of *Id2*^{-/-}*Myd88*^{-/-} mice (Fig. 6d). These data collectively suggest that TLR signals in general are critical for CD11c^{hi}CD11b^{hi} LPDC-mediated activation of acquired immunity.

DISCUSSION

In this work we have demonstrated the unique characteristics of CD11c^{hi}CD11b^{hi} TLR5-expressing LPDCs. It is noteworthy that TLR5 activation by flagellin triggered CD11c^{hi}CD11b^{hi} LPDC-mediated adaptive immune responses. Studies have shown that adjuvant effects are associated with the induction of protective immunity in the intestine. Injection of the ligand for the receptor tyrosine kinase Flt3, which expands DC populations in the intestine, enhances both tolerance and immunity to orally administered antigens^{42,43}. Relative to mice fed antigen alone, those receiving Flt3 ligand and antigen show greater susceptibility to the induction of oral tolerance⁴². However, such oral tolerance is abrogated and immune responses are induced when mice are fed the same antigen with an adjuvant such as IL-1 or cholera toxin⁴³. Such findings indicate that DC activation is a crucial parameter determining whether tolerance or protective immunity is induced in the intestine. In physiological conditions, antigens such as food proteins may be presented by quiescent CD11c^{hi}CD11b^{hi} LPDCs in the absence of inflammation, leading to tolerance. However, when inflammatory stimuli such as flagellin are present, CD11c^{hi}CD11b^{hi} LPDCs will undergo maturation, release inflammatory cytokines and initiate protective acquired immunity.

Commensal bacteria are present at a high density in the intestinal lumen (up to 1×10^{12} bacteria per gram of luminal contents). Most commensal organisms reside outside the layer of mucus that covers the intestinal epithelial cells. Some bacteria penetrate the enterocyte epithelial layer but are rapidly killed by macrophages⁴⁴. However, some commensal bacteria are ingested by DCs, where they survive for several days⁶. Moreover, intraepithelial DCs send protrusions into the lumen of the small intestine in a CX3CR1-dependent way and directly sample luminal commensal bacteria^{45,46}. Commensal bacteria-loaded DCs mediate the induction of natural secretory IgA²⁷, and germ-free mice have a profound deficiency in IgA production in the intestinal mucosa⁴⁴. Thus, the presence of intestinal microbiota influences IgA production in the intestine. As the induction of B220-IgA⁺ plasma cells was impaired in *Id2*^{-/-}*Tlr5*^{-/-} mice and was almost completely abrogated in *Id2*^{-/-}*Myd88*^{-/-} mice, GALT-independent IgA production seems to be mediated by TLR stimulation. These results indicate that TLRs represent a 'missing link' between commensal bacteria and IgA synthesis in the lamina propria.

The ability to synthesize retinoic acid enables CD11c^{hi}CD11b^{hi} LPDCs to modulate various immune response parameters. CD11c^{hi}CD11b^{hi} LPDCs induced IgA⁺ cell differentiation without T cell help in a retinoic acid-dependent way. In the process, CD11c^{hi}CD11b^{hi} LPDCs also promoted the upregulation of CCR9 expression on B cells. Notably, IgA⁺ plasma cells had high expression CCR9 in the lamina propria of GALT-deficient *Id2*^{-/-} mice. These results were unexpected, because GALT DCs are believed to 'imprint' gut tropism on lymphocytes. The ability of CD11c^{hi}CD11b^{hi} LPDCs

to induce CCR9 on differentiated IgA⁺ plasma cells may promote retention in the lamina propria, as the CCR9 ligand CCL25 is abundantly secreted by the crypt epithelium²¹. Although previous studies have shown that retinoic acid negatively regulates T_H-17 cell differentiation, here we have shown that the effect of retinoic acid on T helper cell differentiation depended strictly on its concentration. It is difficult to determine the local concentrations of retinoic acid secreted by CD11c^{hi}CD11b^{hi} LPDCs. However, studies intensively examining the concentration of retinoic acid secreted by GALT DCs in the work of T cell 'imprinting' have shown that 1 nM of retinoic acid is the optimum concentration for the induction of gut-homing receptors on T cells⁴¹. Notably, high concentrations of retinoic acid inhibited the differentiation of both T_H1 and T_H-17 cells, which suggested that the inhibitory effect of high concentrations of retinoic acid is not specific for T_H-17 polarization. Such observations indicate that the effect of retinoic acid on T_H-17 cell differentiation should be considered more cautiously. In any case, like the CD11c^{hi}CD11b^{hi} LPDC-induced differentiation of IgA⁺ plasma cells, T_H-17 cell differentiation required retinoic acid. Unlike other conventional DCs, LPDCs can induce the differentiation of antigen-specific T_H-17 cells as well as T_H1 cells in response to TLR stimulation. The ability to produce retinoic acid may support this unique function of CD11c^{hi}CD11b^{hi} LPDCs.

We conclude that CD11c^{hi}CD11b^{hi} LPDCs may work against bacterial infection by inducing 'local' IgA secretion and 'systemic' T helper cell responses through TLR stimulation. As IL-17 can influence cytokine production by a wide range of cell types and can induce the activation and migration of neutrophils⁴⁷, CD11c^{hi}CD11b^{hi} LPDCs and T_H-17 cells may modulate the pathogenesis of intestinal bowel diseases such as Crohn's disease. In addition, the ability of CD11c^{hi}CD11b^{hi} LPDCs to induce the differentiation of T_H1 and IgA⁺ cells suggests that CD11c^{hi}CD11b^{hi} LPDCs might be useful targets of mucosal vaccination.

METHODS

Mice. *Tlr4*^{-/-} (C57BL/6) mice, *Tlr5*^{-/-} mice (C57BL/6), *Id2*^{-/-} mice and *Myd88*^{-/-} mice have been described^{18,48}. *Il6*^{-/-} mice (C57BL/6) and OT-II-transgenic mice (C57BL/6) were provided by M. Kopf⁴⁹ and W.R. Heath⁵⁰, respectively. All animal experiments were done with the approval of the Animal Research Committee of the Research Institute for Microbial Diseases at Osaka University.

Reagents. LPS, flagellin and CpG oligodeoxynucleotides (ODN 1668) were purified as described¹⁸. *S. typhimurium* flagellin was from Invivogen. All-trans retinoic acid (Sigma) was dissolved in dimethyl sulfoxide, was stored at -80 °C with light interception and was added to cultures at a final concentration of 1 nM. LE540 (Wako) was dissolved in dimethyl sulfoxide and was added to cultures at a final concentration of 1 μM.

Cells. Segments of the small intestine were treated for 30 min at 37 °C with PBS containing 10% (vol/vol) FCS, HEPES (20 mM), pH 7.4, penicillin (100 U/ml), streptomycin (100 μg/ml), sodium pyruvate (1 mM), EDTA (10 mM) and polymyxin B (10 μg/ml; Calbiochem) for removal of epithelial cells, then were washed extensively with PBS. Segments of the small intestine and spleen were digested for 45–90 min with continuous stirring at 37 °C with collagenase D (400 Mandl units/ml; Roche) and DNase I (10 μg/ml; Roche) in RPMI 1640 medium plus 10% (vol/vol) FCS. EDTA was added (final concentration, 10 mM) and cell suspensions were incubated for an additional 5 min at 37 °C. Cells were spun through a 17.5% (wt/vol) solution of Accudenz (Accurate Chemical & Scientific) for enrichment for DCs. The cells obtained were incubated with fluorescein isothiocyanate-conjugated antibody to CD11b (anti-CD11b; M170; 557396) and phycoerythrin-conjugated anti-CD11c (HL3; 557401; both from BD Pharmingen) after blockade of Fc receptors. DC subsets were sorted on the basis of their expression of CD11c and CD11b with a FACS Vantage SE or FACS Aria (BD Biosciences). The purity of the sorted DCs

